Supplementary Information

SUPPLEMENTARY FIGURES

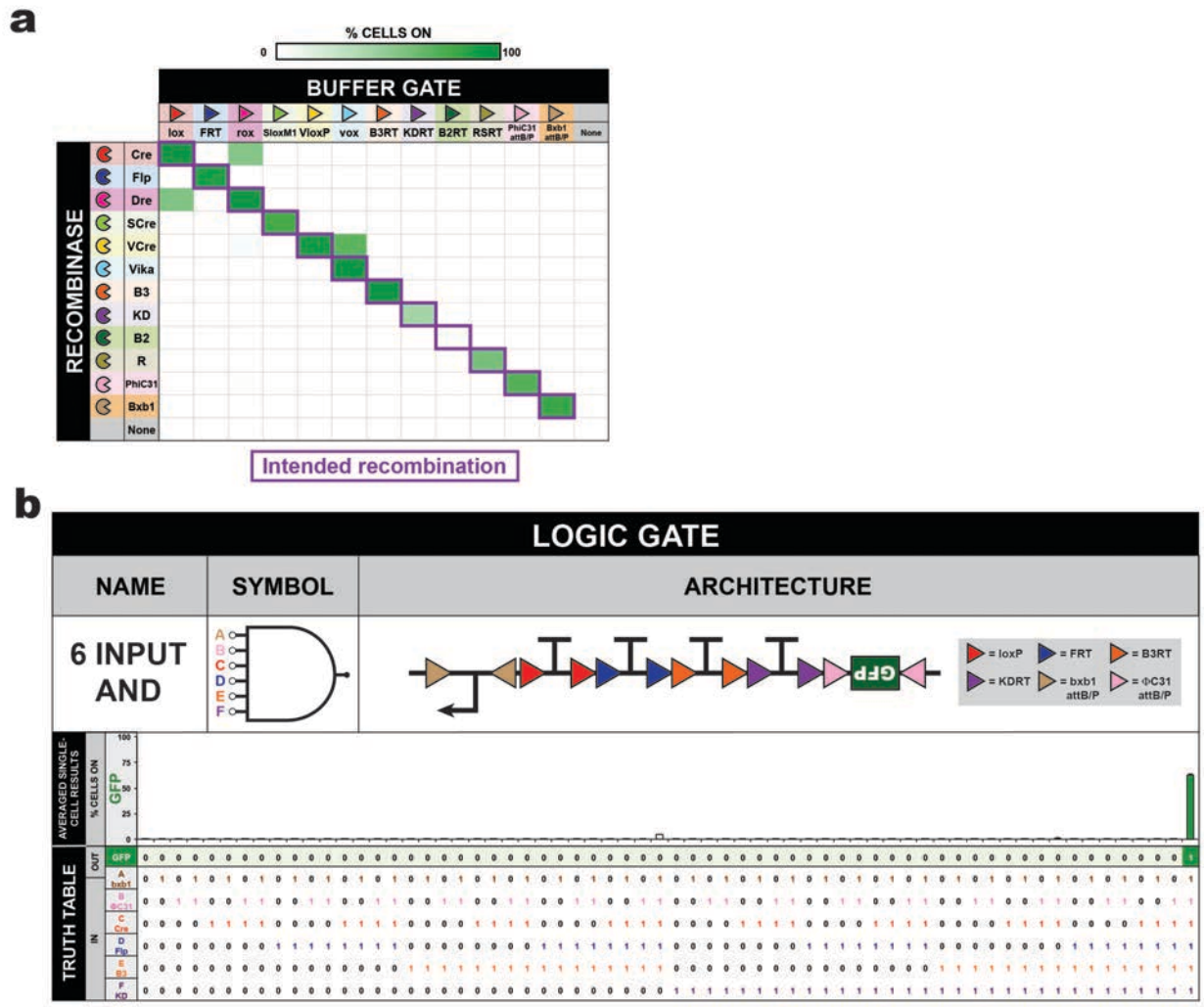

Supplementary Figure 1. Orthogonal site-specific tyrosine recombinases and serine integrases enable implementation of multi-input AND gates in mammalian cells.

(a) Recombinases are tested for their recombination efficiency and orthogonality on all BUF logic reporters. (b) A 6-input AND-gate that produces GFP when all inputs are present. % Cells ON calculated from n = 3 transfected cell cultures; a.u. = arbitrary units. Error bars represent standard error of the mean.

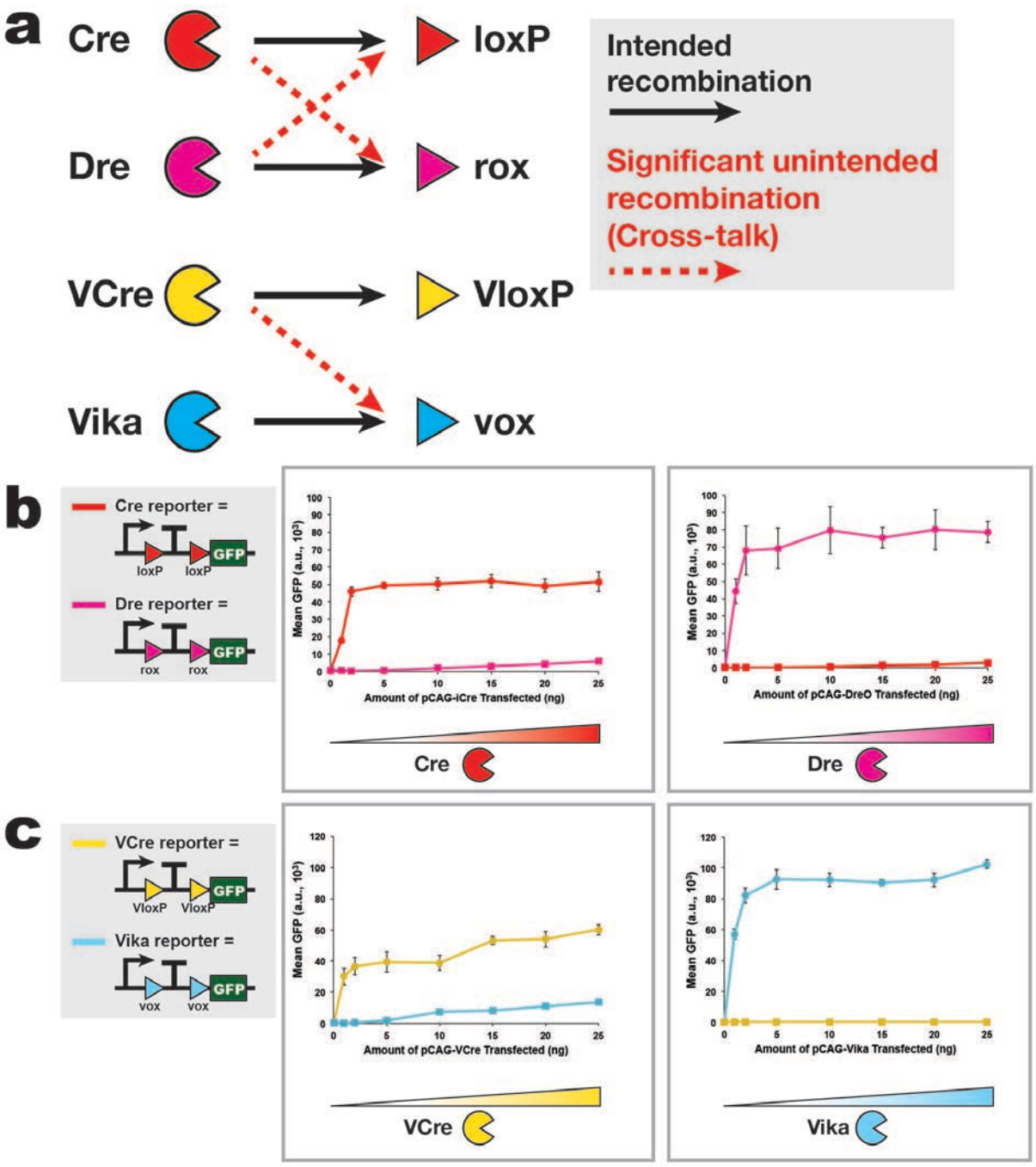

Supplementary Figure 2. Recombinase cross-reactivity dose-response profile of Cre, Dre, VCre and Vika

(a) Summary of intended and unintended recombination of Cre, Dre, VCre and Vika site-specific recombinases. Cre and Dre are mutually cross-reactive, whereas VCre can recombine Vika's recombination sites, but not the other way around. (b) Dose-response profile of Cre (*left*) and Dre (*right*) on both Cre and Dre reporter constructs. (c) Dose-response profile of VCre (*left*) and Vika (*right*) on both VCre and Vika reporter

constructs. Mean fluorescence intensity is plotted from n = 3 transfected cell cultures; a.u. = arbitrary units. Error bars represent standard error of the mean.

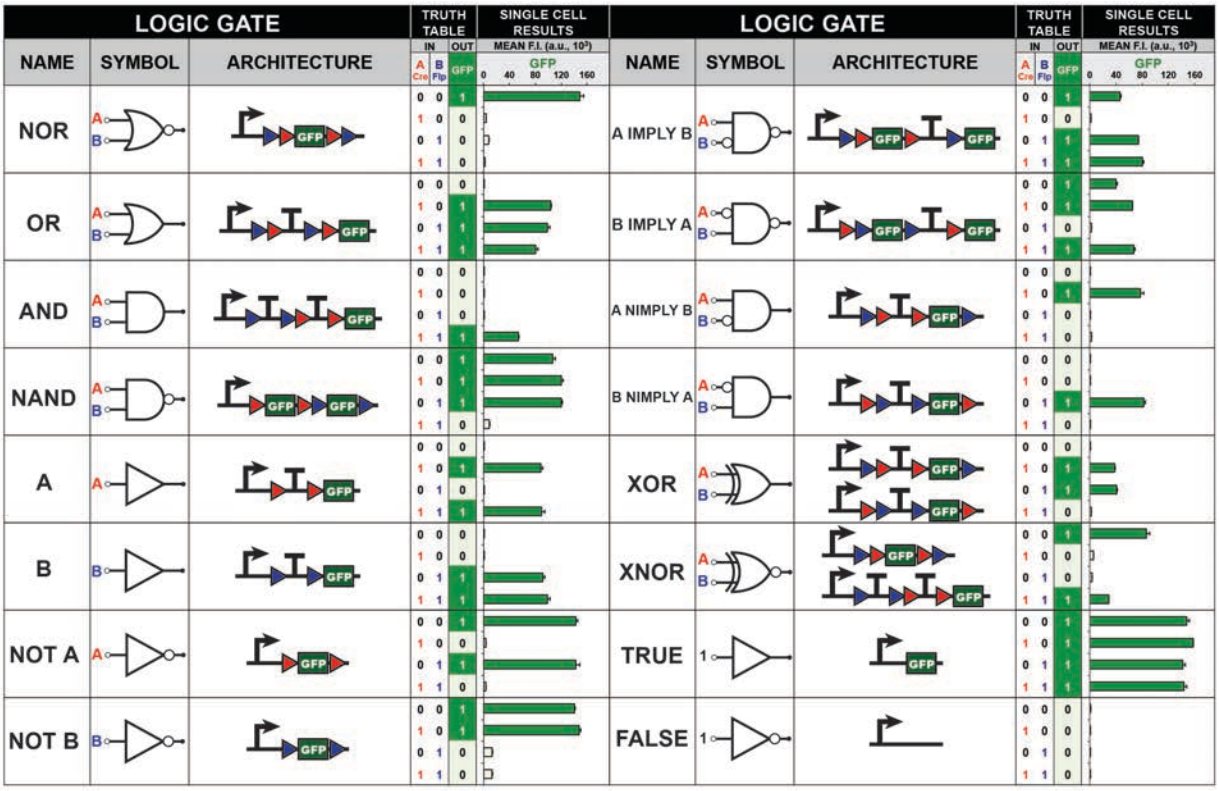

Supplementary Figure 3. Recombinase-based 2-input, 1-output Boolean logic gates using Cre and Flp recombinases

Recombination sites for Cre and Flp are placed around termination sequences or GFP to enable or disable GFP expression. In this fashion all sixteen Boolean logic functions were created in mammalian cells.

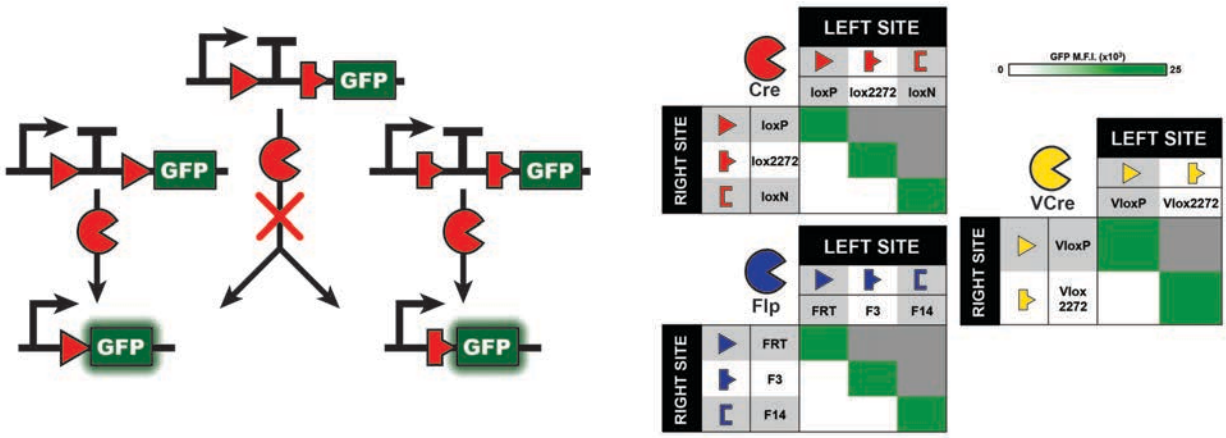

Supplementary Figure 4. Heterospecific recombination sites
Heterospecific recombination sites for Cre, Flp, and VCre are placed around termination sequences before a GFP sequence.

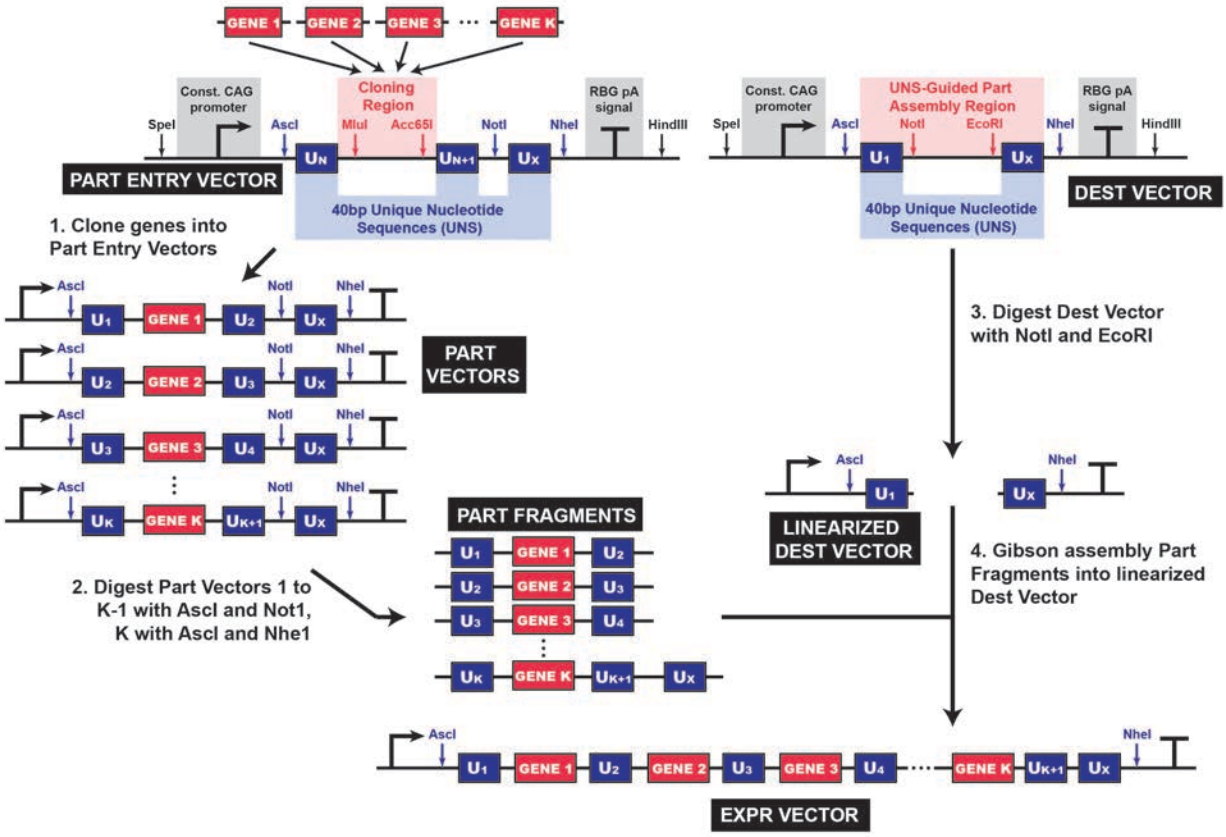

Supplementary Figure 5. Unique Nucleotide Sequence guided assembly provides a fast and modular approach for creating DNA constructs

Genes are first cloned into part entry vectors that contain 40bp unique nucleotide sequences (UNSes). These part vectors are then digested with either Asc1+Not1 or Asc1+Nhe1 restriction endonucleases to expose UNSes. The part fragments are then gel purified and assembled into a linearized destination vector using Gibson isothermal assembly. Details are described in [1].

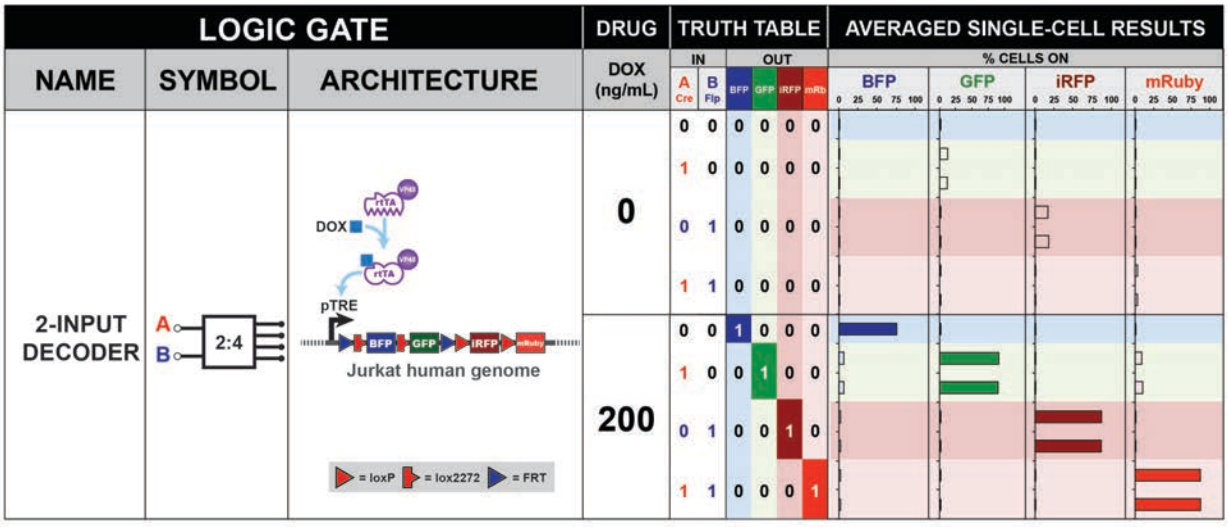

Supplementary Figure 6. 2-input BLADE platform can produce four distinct output functions based on two inputs

Integrated 2-input BLADE decoder with tagBFP, EGFP, iRFP720, and mRuby2 as addresses Z_{00}, Z_{10}, Z_{01}, and Z_{11} respectively. Plasmids constitutively expressing Cre and/or Flp are then stably integrated in. Three days of doxycycline (DOX) treatment is used to permit the rtTA-VP48 protein to bind to the tetracycline response elements promoter (pTRE) to activate gene expression. % Cells ON is plotted of either n = 1 or n = 2 integrations. a.u. = arbitrary units.

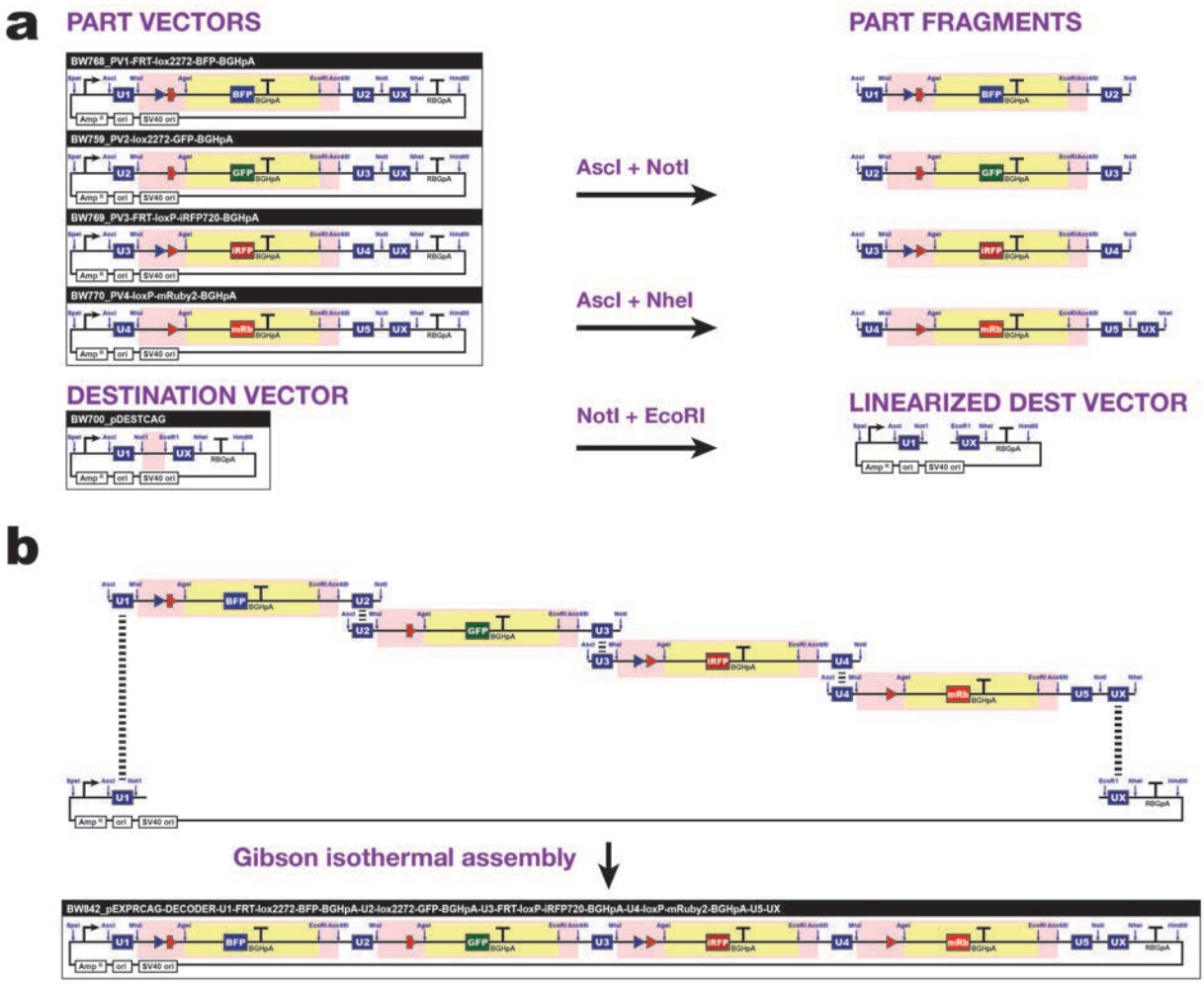

Supplementary Figure 7. Construction of two-input BLADE constructs using Unique Nucleotide Sequence Guided Assembly

(a) To create a two-input BLADE construct, part vectors are created that contain output states for each address. The part vectors, along with a destination (DEST) vector, are digested and gel purified to expose unique nucleotide sequences (UNSes). (b) The part fragments and linearized destination vector are then assembled together in order of UNS via Gibson isothermal assembly to form the final expression vector.

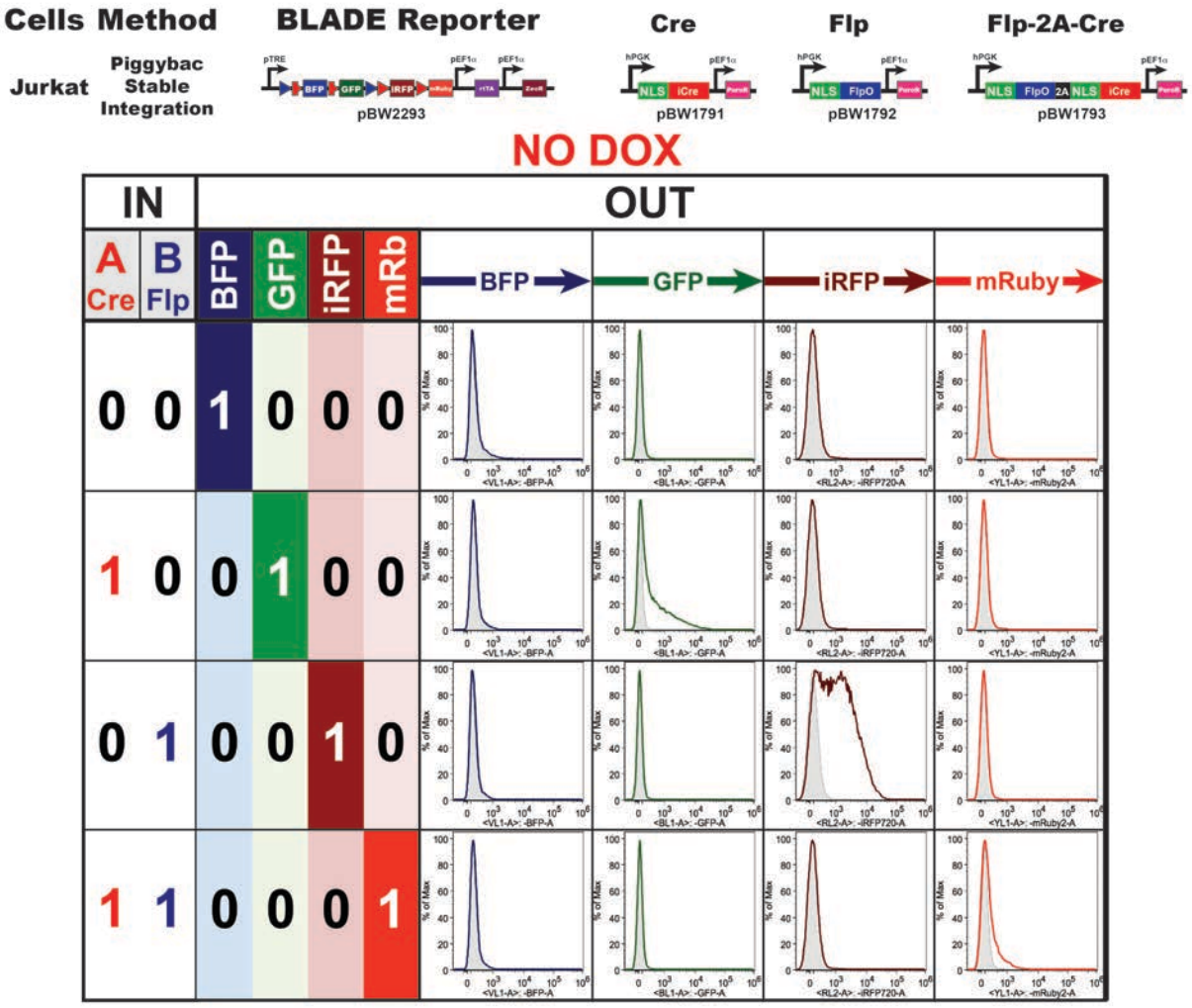

Supplementary Figure 8. Fluorescence histograms for 2-input decoder in non-induced Jurkat T lymphocytes

2-input decoder produces a particular fluorescent protein for each row of the truth table. Grey histograms indicate wildtype Jurkat cells, unshaded colored histograms indicate OFF states and shaded colored histograms indicate ON states. Data is shown for one of the integrations.

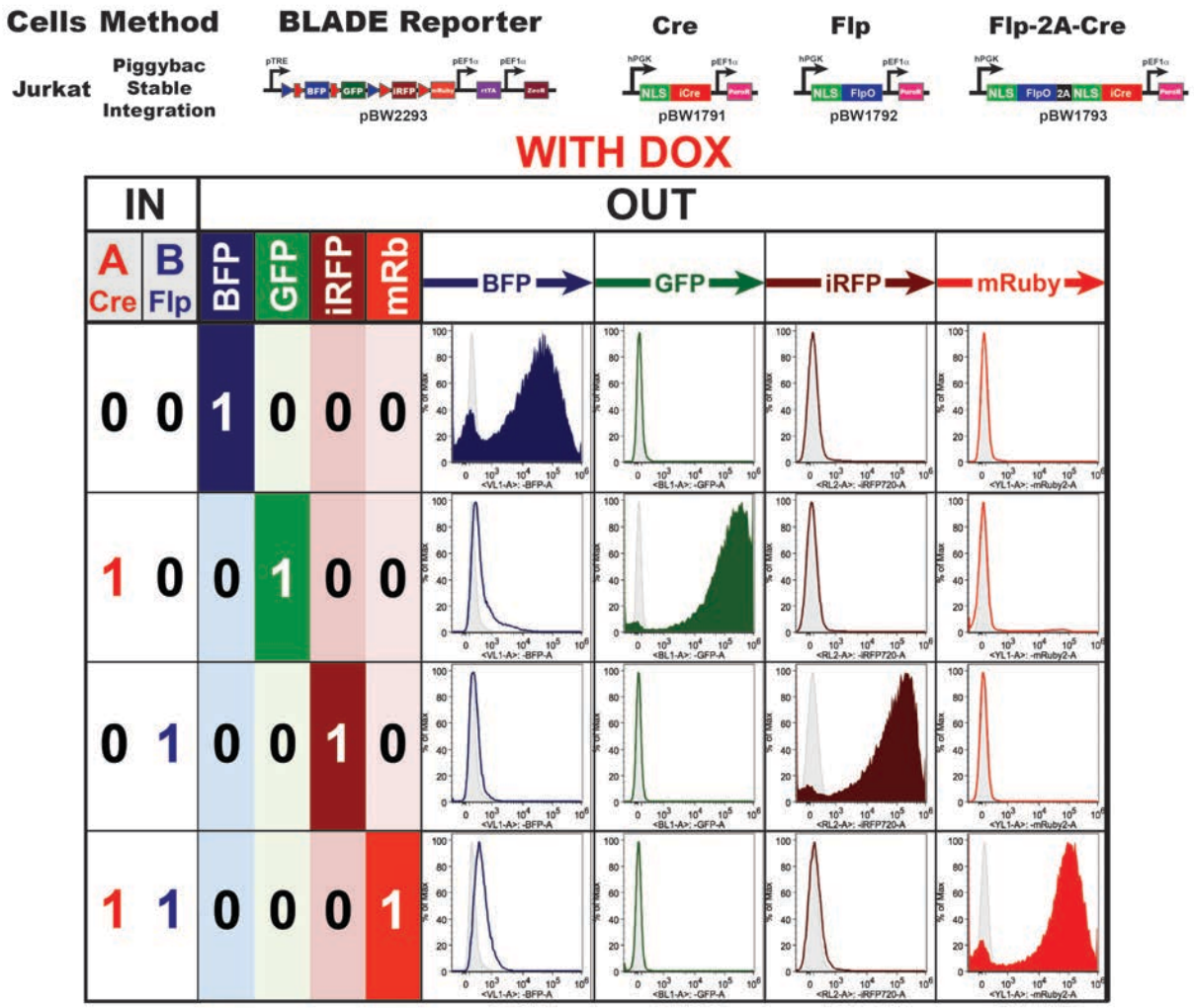

Supplementary Figure 9. Fluorescence histograms for 2-input decoder in doxycycline-induced Jurkat T lymphocytes

2-input decoder produces a particular fluorescent protein for each row of the truth table. Grey histograms indicate wildtype Jurkat cells, unshaded colored histograms indicate OFF states and shaded colored histograms indicate ON states. Data is shown for one of the integrations.

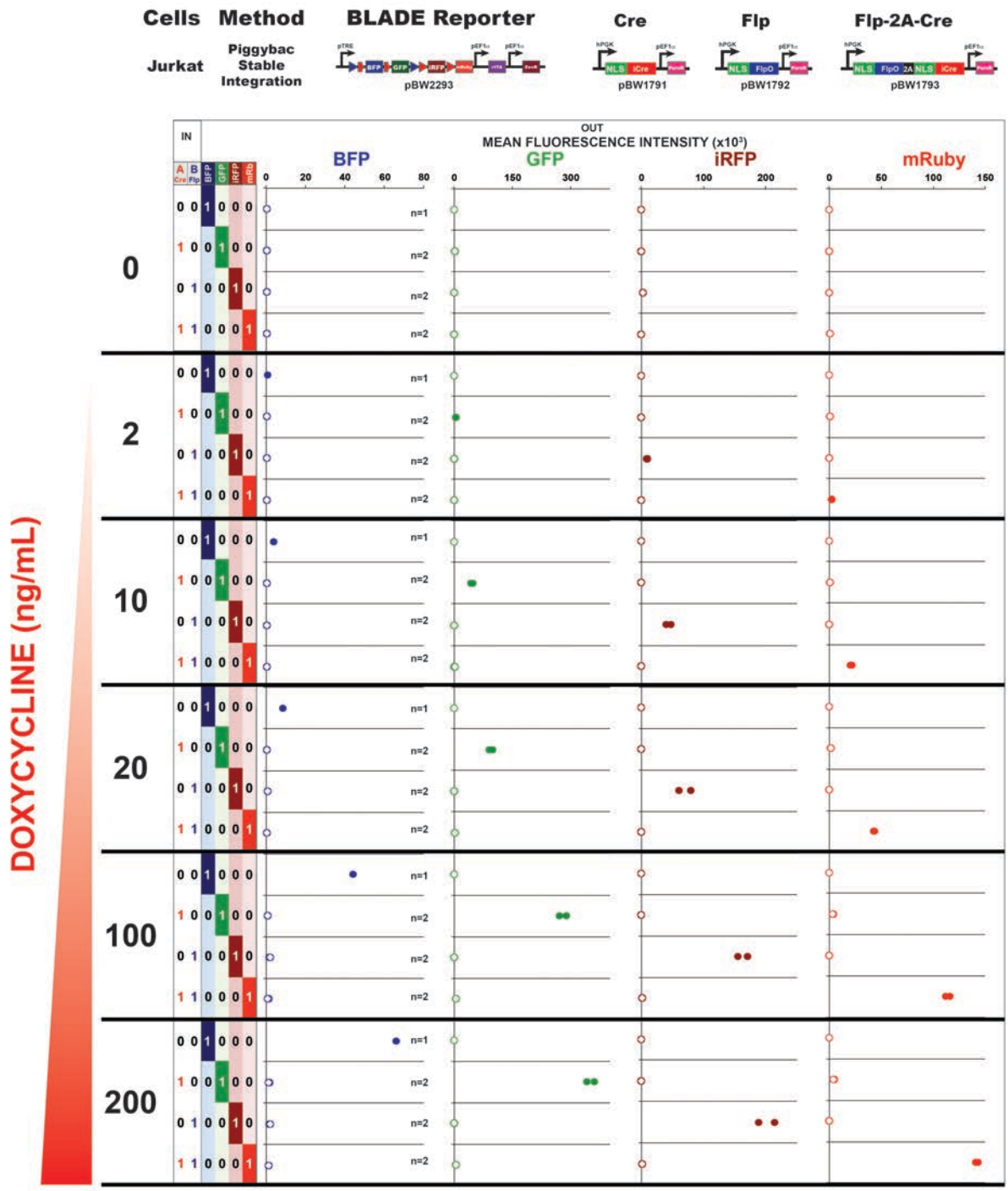

Supplementary Figure 10. Output response of integrated doxycycline-inducible decoder in Jurkat T cells can be easily modulated by dosage of doxycycline.
2-input decoder produces a particular fluorescent protein for each row of the truth table. Unshaded colored dots indicate OFF states and shaded colored dots indicate ON states. Data is indicated for number of replicate integrations (n=1 or n=2) plotted.

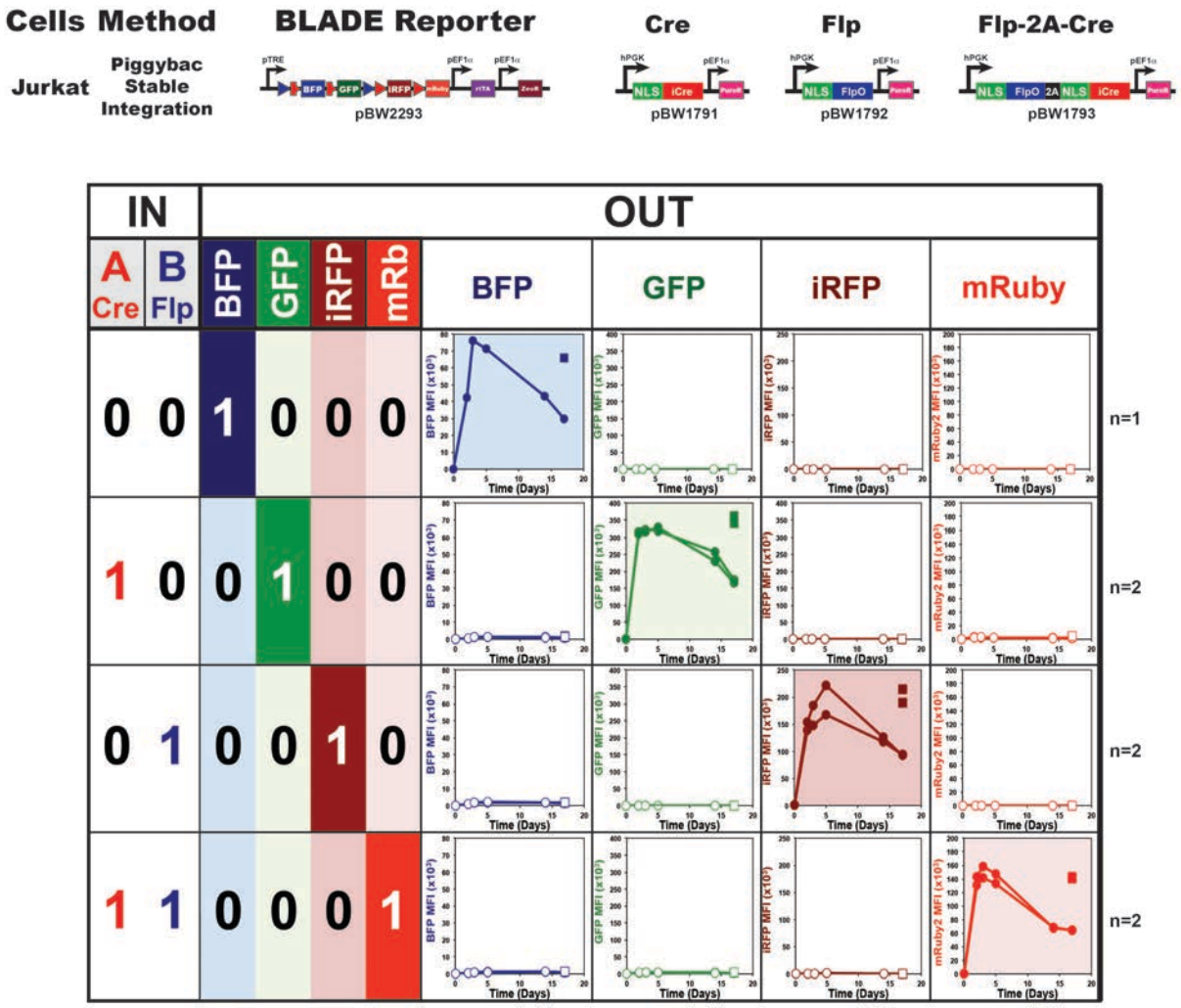

Supplementary Figure 11. Functionality of integrated doxycycline decoder in Jurkat T cells can be maintained over a couple weeks.

2-input decoder produces a particular fluorescent protein for each row of the truth table. Unshaded colored circles indicate OFF states and shaded colored circles indicate ON states; cells here were maintained with doxycycline induction starting from day 0. Unshaded colored squares indicate OFF states and shaded colored squares indicate ON states; cells here were maintained with doxycycline induction starting from day 14 and were not induced with doxycycline prior to that point. Data is indicated for number of replicate integrations (n=1 or n=2) plotted.

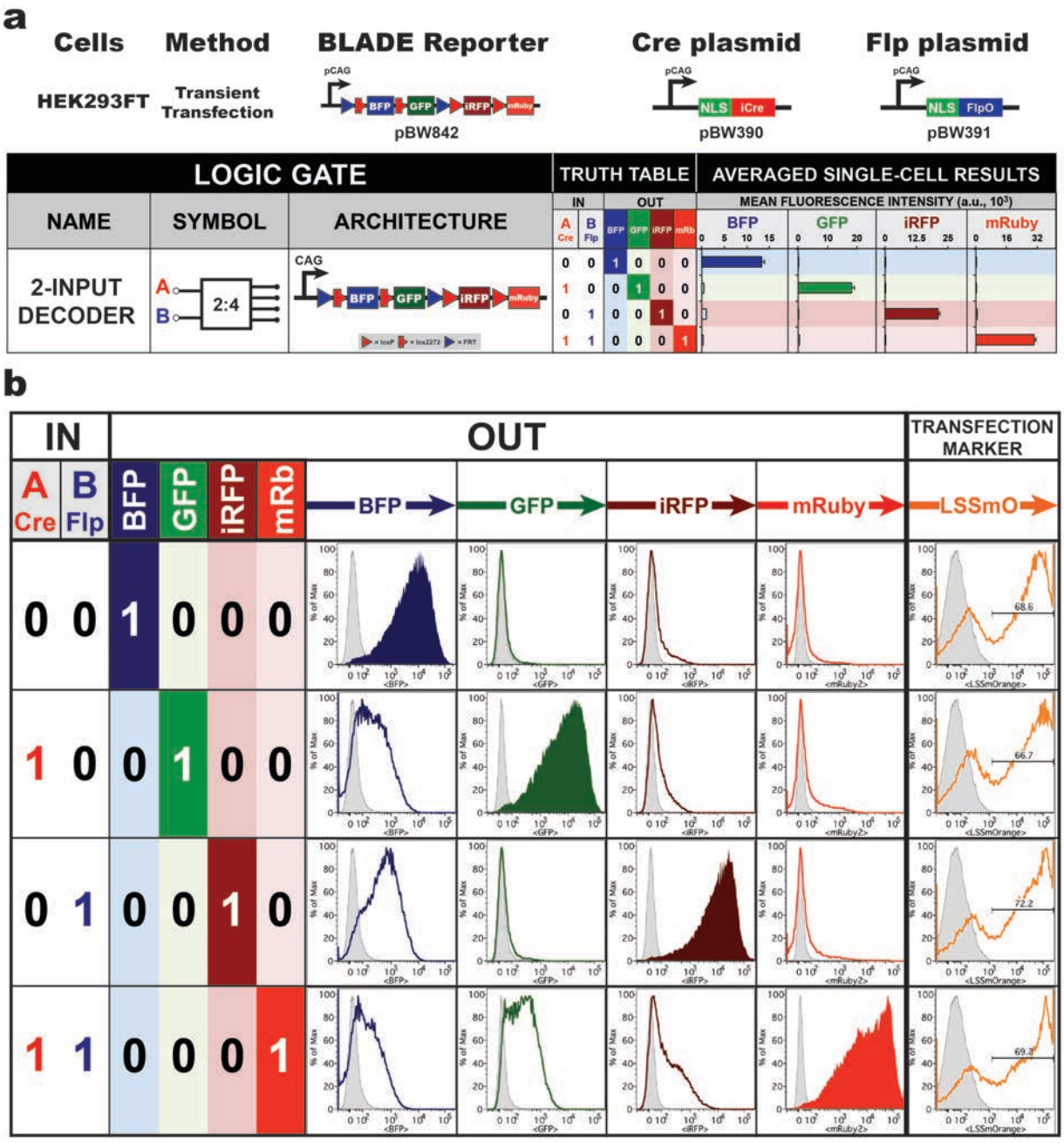

Supplementary Figure 12. Fluorescence bar charts and histograms for 2-input decoder in HEK293FT cells

2-input decoder produces a particular fluorescent protein for each row of the truth table. (a) 2-input BLADE template with tagBFP, EGFP, iRFP720, and mRuby2 as addresses Z_{00}, Z_{10}, Z_{01}, and Z_{11} respectively. Mean fluorescence intensity from n = 3 independent transfections. a.u. = arbitrary units. Error bars represent standard error of the mean. (b) Grey histograms indicate wildtype HEK293FT, unshaded colored histograms indicate OFF states and shaded colored histograms indicate ON states. Data is shown for one of the three replicate transfected cell cultures.

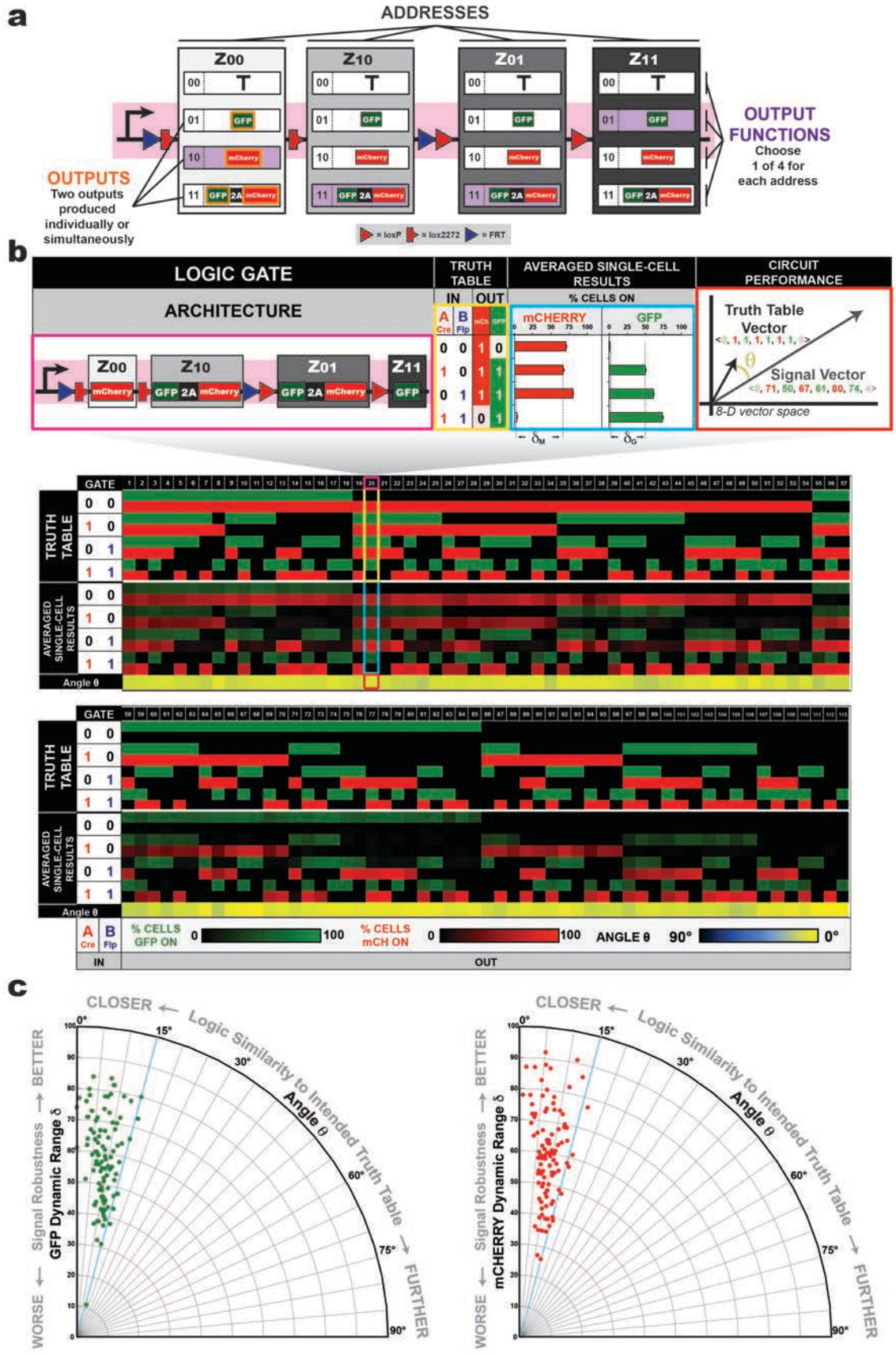
a
ADDRESSES
Z00
Z10
Z01
Z11
00 T
01 GFP
10 mCherry
11 GFP 2A mCherry
OUTPUTS
Two outputs produced individually or simultaneously
OUTPUT FUNCTIONS
Choose 1 of 4 for each address
= loxP = lox2272 = FRT
b
LOGIC GATE
ARCHITECTURE
TRUTH TABLE
IN
OUT
A Cre
B Flp
mCh
GFP
AVERAGED SINGLE-CELL RESULTS
% CELLS ON
mCHERRY
GFP
CIRCUIT PERFORMANCE
Truth Table Vector
Signal Vector
8-D vector space
GATE
TRUTH TABLE
AVERAGED SINGLE-CELL RESULTS
Angle θ
% CELLS GFP ON
% CELLS mCH ON
ANGLE θ
90°
0°
c
CLOSER ← Logic Similarity to Intended Truth Table → FURTHER
WORSE ← Signal Robustness → BETTER
GFP Dynamic Range δ
mCHERRY Dynamic Range δ
Angle θ
15°
30°
60°
75°
90°

Supplementary Figure 13. One hundred and thirteen distinct gene circuits with up to two inputs and two outputs implemented using the 2-input BLADE template
(a) To generate 2-input, 2-ouput circuits, a 2-input BLADE template can be configured with different combinations of output functions: zero-output (transcription termination sequence), one-output (GFP or mCherry) or two-output (GFP-T2A-mCherry). (b) A diverse library of >100 gene circuits, each shown as an individual column with predicted truth table GFP/mCherry ON/OFF behavior (black = no output, green = GFP ON, red = mCherry ON) and corresponding experimental averaged single-cell results obtained from flow cytometry. (c) Angles between each Signal Vector and corresponding Intended Truth Table Vectors are plotted versus worst-case dynamic range values for GFP (δ_G) and mCherry (δ_M) signals. Shown above is an expanded view of one of the logic gates made using this platform. % Cells ON is calculated from n = 3 transfected cell cultures. Error bars represent standard error of the mean.

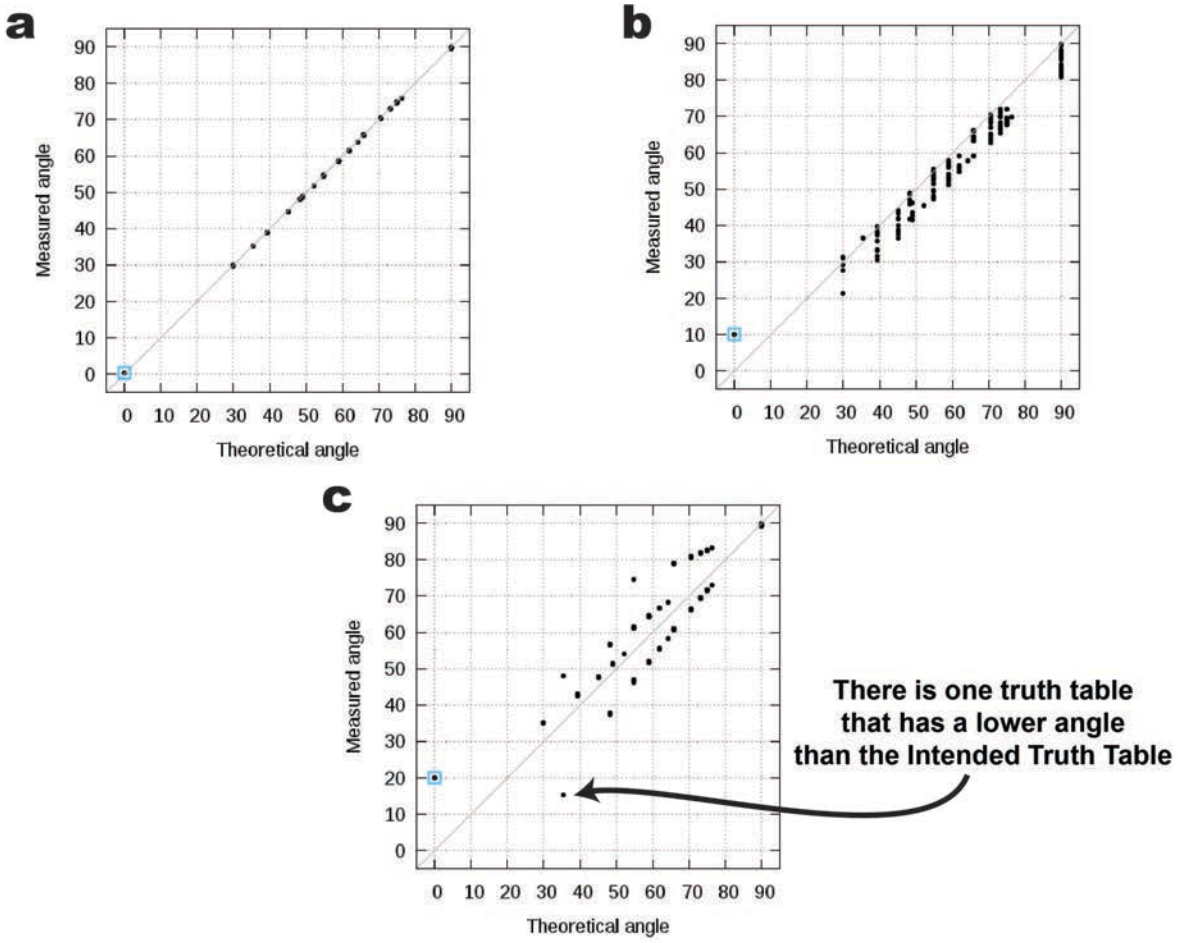

Supplementary Figure 14. Determination of angular global rank amongst possible 255 truth tables for circuits made using the 2-input-2-output BLADE platform

For a particular genetic circuit, angles between the Intended Truth Table vector and all 255 (up to 2-input, up to 2-output, excluding the 0-input-0-output FALSE) truth tables vectors were found (Theoretical Angle), where an angle of zero indicates the intended truth table vector (squared in blue). Similarly, the angles between the signal vector and all possible truth table vectors were found (Measured Angle), where the lowest angle indicates the best truth table match. The global rank n is determined by how many (n) other truth tables were closer than the intended truth table. The first two plots (a) and (b) indicate two circuits (Gate 89 and Gate 71, respectively) that achieved a global rank 0 and VP angle scores around 0° and 10°, respectively. The bottom plot (c) indicates Gate 94, where the signal vector was closer to one other truth table than the intended truth table (VP global rank 1); this circuit had a higher VP angle score as well around 20°.

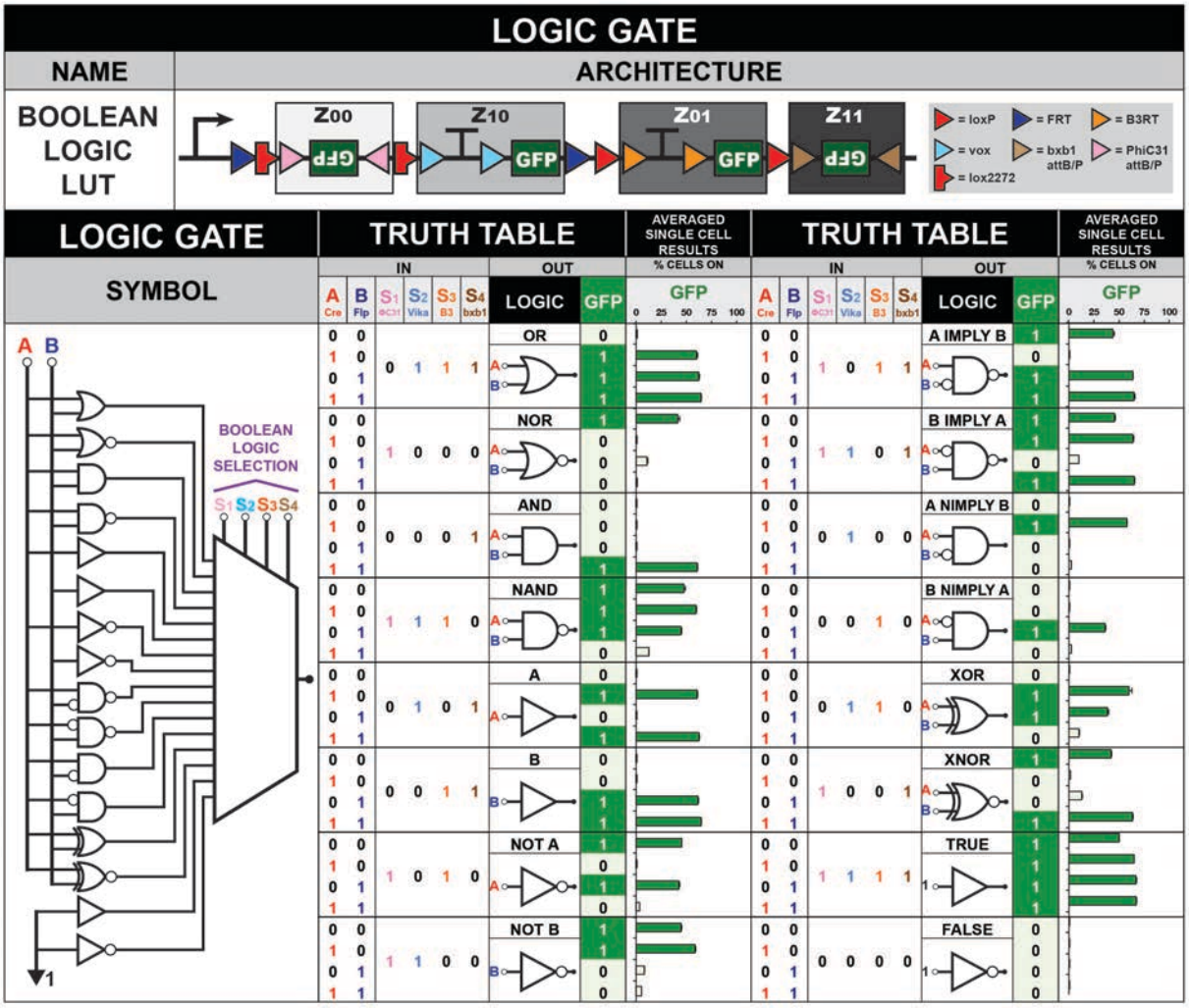

Supplementary Figure 15. Field-programmable storage and retrieval of logic and memory using a Boolean Logic Look-Up Table (LUT)

The Boolean Logic LUT is a six-input-one-output genetic device that receives two data inputs, A and B, and is controlled by four select inputs, S_1, S_2, S_3, and S_4, producing an output of GFP. The select inputs are used to change data input-output behavior; each combination configures the device to any of the sixteen Boolean logic gates. F.I. = fluorescence intensity from n = 3 transfected cell cultures. Error bars represent standard error of the mean.

a

LOGIC GATE	
NAME	ARCHITECTURE
BOOLEAN LOGIC LUT	

LOGIC GATE	TRUTH TABLE									SINGLE CELL RESULTS	TRUTH TABLE									SINGLE CELL RESULTS
SYMBOL	IN						OUT			MEAN F.I.(a.u., 10^3)	IN						OUT			MEAN F.I.(a.u., 10^3)
	A Cre	B Flp	S_1 Dre	S_2 Vika	S_3 B3	S_4 tCre	LOGIC	GFP		GFP 0 10 20 30	A Cre	B Flp	S_1 Dre	S_2 Vika	S_3 B3	S_4 tCre	LOGIC	GFP		GFP 0 10 20 30
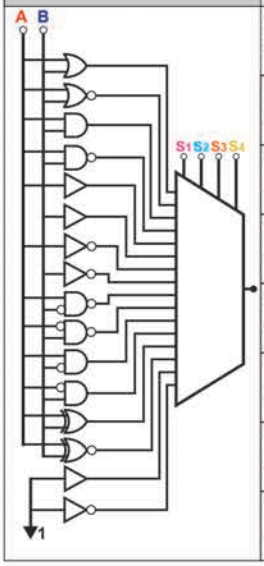	0	0	0	1	1	1	OR	0			0	0	1	0	1	1	A IMPLY B	1		
	1	0						1			1	0						0		
	0	1						1			0	1						1		
	1	1						1			1	1						1		
	0	0	1	0	0	0	NOR	1			0	0	1	1	0	1	B IMPLY A	1		
	1	0						0			1	0						1		
	0	1						0			0	1						0		
	1	1						0			1	1						1		
	0	0	0	0	0	1	AND	0			0	0	0	1	0	0	A NIMPLY B	0		
	1	0						0			1	0						1		
	0	1						0			0	1						0		
	1	1						1			1	1						0		
	0	0	1	1	1	0	NAND	1			0	0	0	0	1	0	B NIMPLY A	0		
	1	0						1			1	0						0		
	0	1						1			0	1						1		
	1	1						1			1	1						0		
	0	0	0	1	0	1	A	0			0	0	0	1	1	0	XOR	0		
	1	0						1			1	0						1		
	0	1						0			0	1						1		
	1	1						1			1	1						0		
	0	0	0	0	1	1	B	0			0	0	1	0	0	1	XNOR	1		
	1	0						0			1	0						0		
	0	1						1			0	1						0		
	1	1						1			1	1						1		
	0	0	1	0	1	0	NOT A	1			0	0	1	1	1	1	TRUE	1		
	1	0						0			1	0						1		
	0	1						1			0	1						1		
	1	1						0			1	1						1		
	0	0	1	1	0	0	NOT B	1			0	0	0	0	0	0	FALSE	0		
	1	0						1			1	0						0		
	0	1						0			0	1						0		
	1	1						0			1	1						0		

b

LOGIC GATE	
NAME	ARCHITECTURE
BOOLEAN LOGIC LUT (Low Dose)	

LOGIC GATE	TRUTH TABLE									SINGLE CELL RESULTS	TRUTH TABLE									SINGLE CELL RESULTS
SYMBOL	IN						OUT			MEAN F.I.(a.u., 10^3)	IN						OUT			MEAN F.I.(a.u., 10^3)
	A Cre	B Flp	S_1 Dre	S_2 Vika	S_3 B3	S_4 tCre	LOGIC	GFP		GFP 0 10 20 30	A Cre	B Flp	S_1 Dre	S_2 Vika	S_3 B3	S_4 tCre	LOGIC	GFP		GFP 0 10 20 30
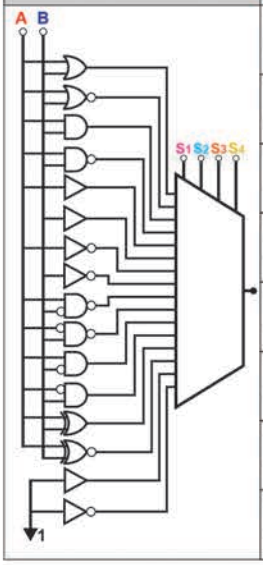	0	0	0	1	1	1	OR	0			0	0	1	0	1	1	A IMPLY B	1		
	1	0						1			1	0						0		
	0	1						1			0	1						1		
	1	1						1			1	1						1		
	0	0	1	0	0	0	NOR	1			0	0	1	1	0	1	B IMPLY A	1		
	1	0						0			1	0						1		
	0	1						0			0	1						0		
	1	1						0			1	1						1		
	0	0	0	0	0	1	AND	0			0	0	0	1	0	0	A NIMPLY B	0		
	1	0						0			1	0						1		
	0	1						0			0	1						0		
	1	1						1			1	1						0		
	0	0	1	1	1	0	NAND	1			0	0	0	0	1	0	B NIMPLY A	0		
	1	0						1			1	0						0		
	0	1						1			0	1						1		
	1	1						1			1	1						0		
	0	0	0	1	0	1	A	0			0	0	0	1	1	0	XOR	0		
	1	0						1			1	0						1		
	0	1						0			0	1						1		
	1	1						1			1	1						0		
	0	0	0	0	1	1	B	0			0	0	1	0	0	1	XNOR	1		
	1	0						0			1	0						0		
	0	1						1			0	1						0		
	1	1						1			1	1						1		
	0	0	1	0	1	0	NOT A	1			0	0	1	1	1	1	TRUE	1		
	1	0						0			1	0						1		
	0	1						1			0	1						1		
	1	1						0			1	1						1		
	0	0	1	1	0	0	NOT B	1			0	0	0	0	0	0	FALSE	0		
	1	0						1			1	0						0		
	0	1						0			0	1						0		
	1	1						0			1	1						0		

Supplementary Figure 16. Alternative versions of the Boolean Logic Look-up Table (LUT)

(a) A Boolean Logic LUT using Dre, Vika, B3 and VCre as select inputs. Red circles indicate areas where cross-reactivity made detectable changes in circuit response. (b) The same Boolean LUT using low amounts of select inputs to reduce cross-reactivity effects of Cre/Dre and VCre/Vika, as noticeably illustrated in the AND and A gates. Red circles indicate areas where cross-reactivity was resolved.

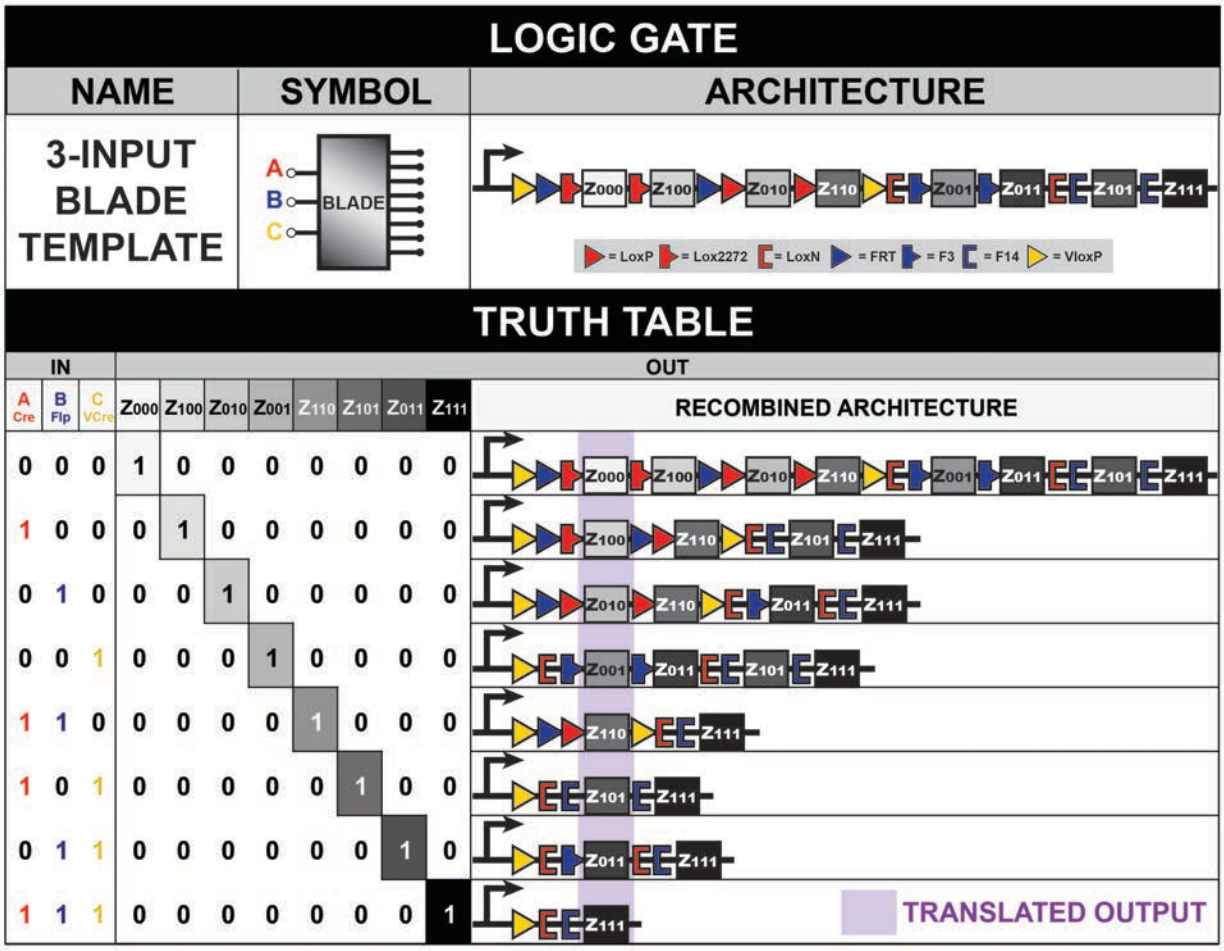

Supplementary Figure 17. The three-input BLADE template can be used to generate eight distinct output functions

The three-input BLADE template uses Cre, Flp, and VCre to generate eight distinct configurations of DNA that each code for a distinct output function.

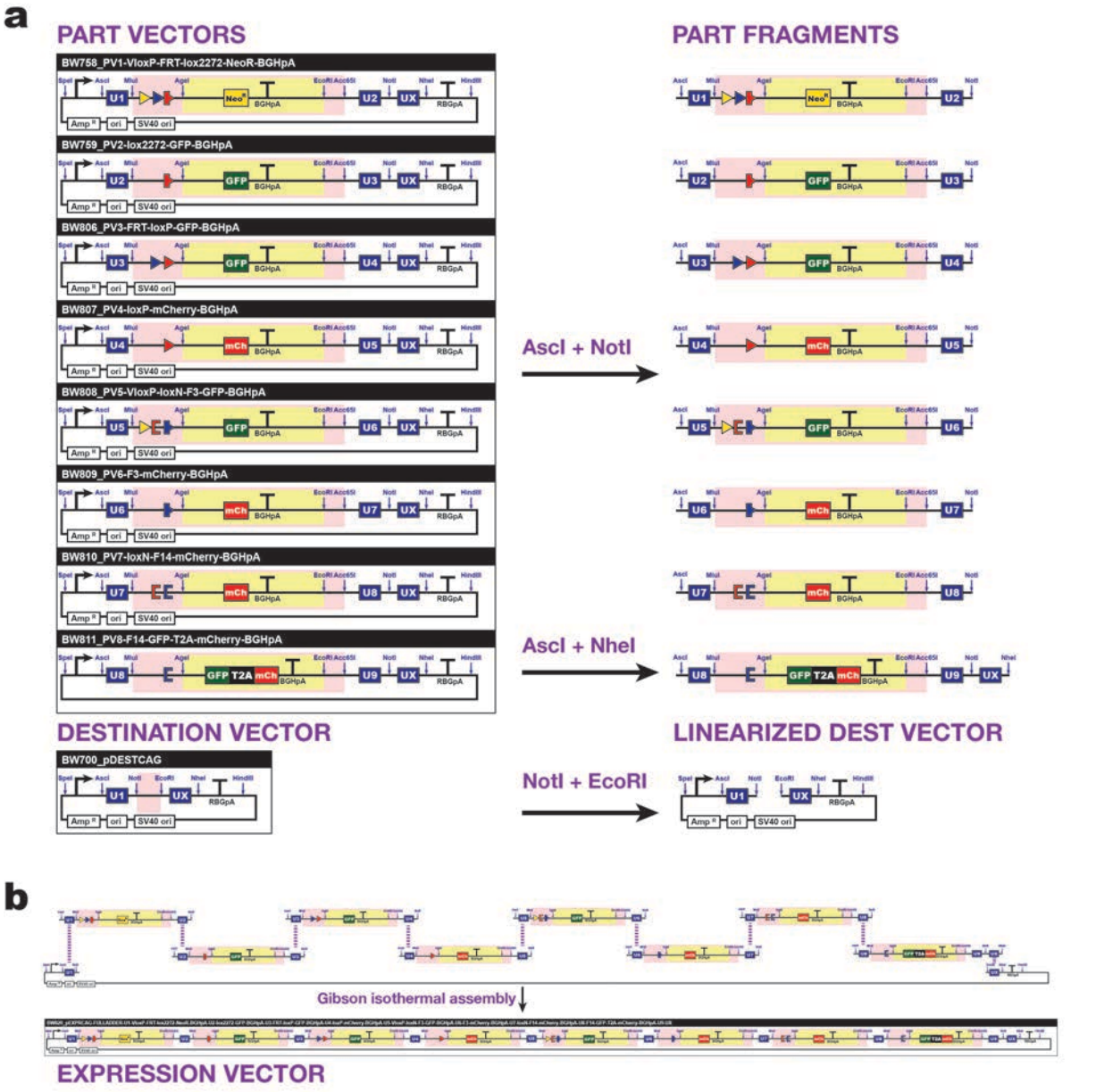

Supplementary Figure 18. Construction of three-input BLADE constructs using Unique Nucleotide Sequence Guided Assembly

(a) To create a three-input BLADE construct, part vectors are created that contain output states for each address. The part vectors, along with a destination (DEST) vector, are digested and gel purified to expose unique nucleotide sequences (UNSes). (b) The part fragments and linearized destination vector are then assembled together in order of UNS via Gibson isothermal assembly to form the final expression vector.

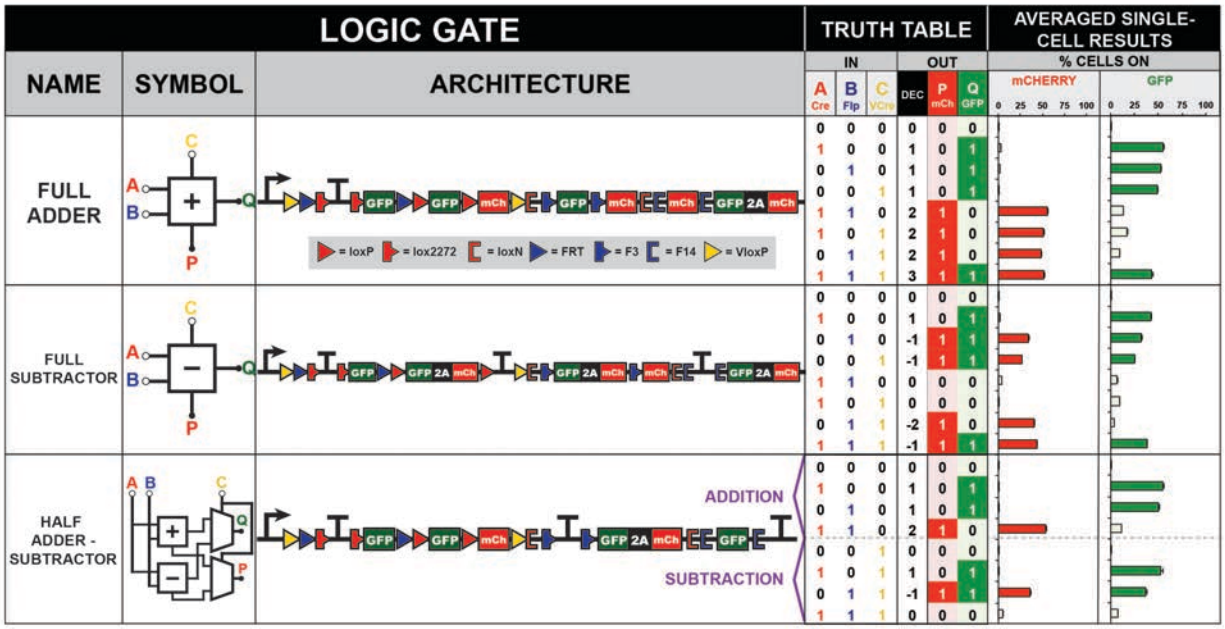

Supplementary Figure 19. A 3-input BLADE template can be applied to create 3-input arithmetic computational circuits

(a) The 3-input BLADE template can receive up to three inputs and produce eight distinct output functions. (b) Three 3-input-2-output binary arithmetic computational circuits made using the 3-input BLADE template. The full adder can add A + B + C while the full subtractor calculates A – B – C. For addition, input C, output P, and output Q represent Carry In, Carry Out and Sum, respectively. For subtraction, input C, output P, and output Q signify Borrow In, Borrow Out and Difference, respectively. The half adder-subtractor performs either binary addition of A + B or binary subtraction of A – B depending on the presence of select input C. % Cells ON is calculated from n = 3 transfected cell cultures. Error bars represent standard error of the mean.

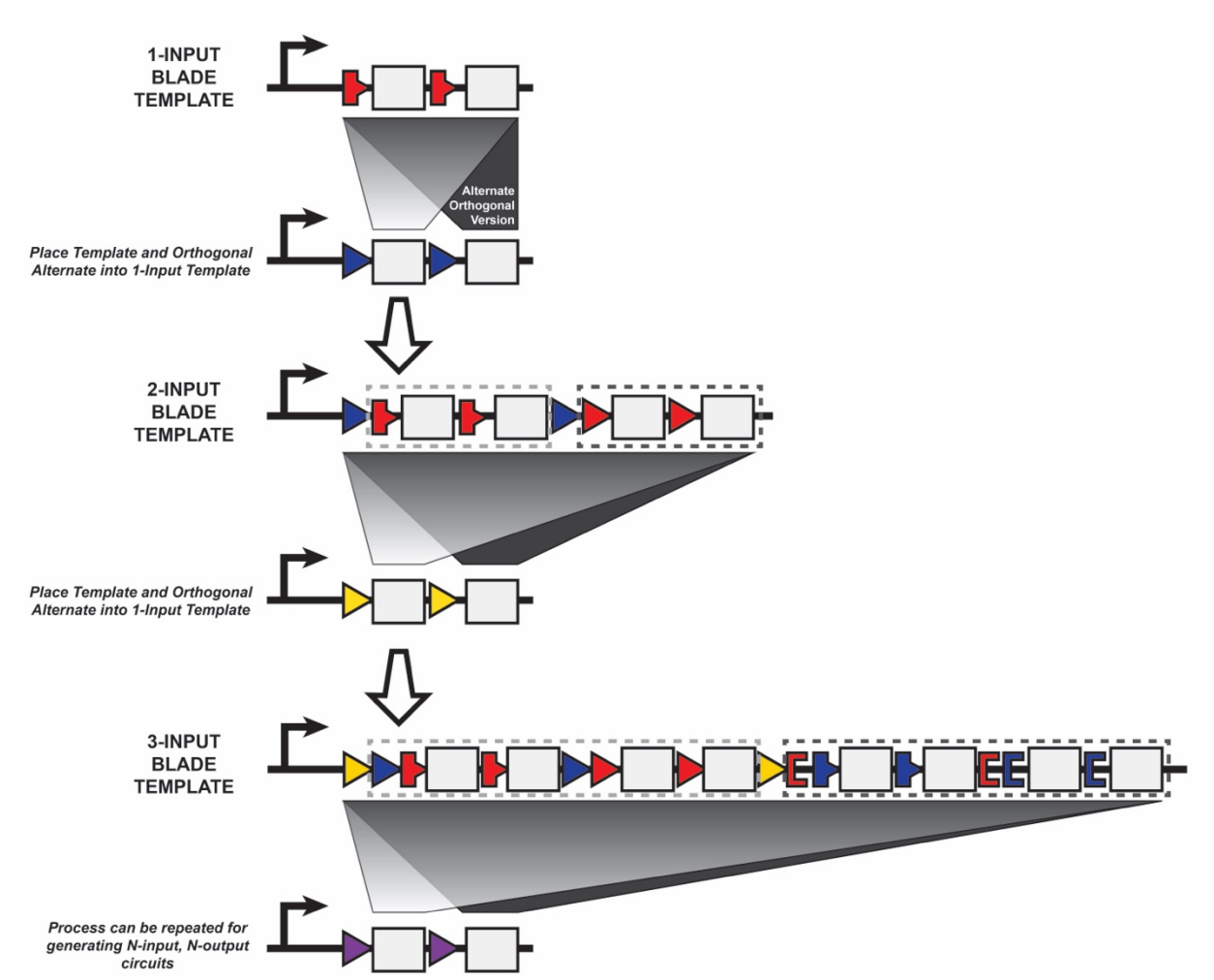

Supplementary Figure 20. Recursive construction of BLADE templates to form up to N-input, N-output combinatorial logic

A BLADE template with and an alternate orthogonal version can be placed into a 1-input BLADE template to increase the input order by one. This approach can be repeated for generating N-input, M-output logic with 2^N addresses.

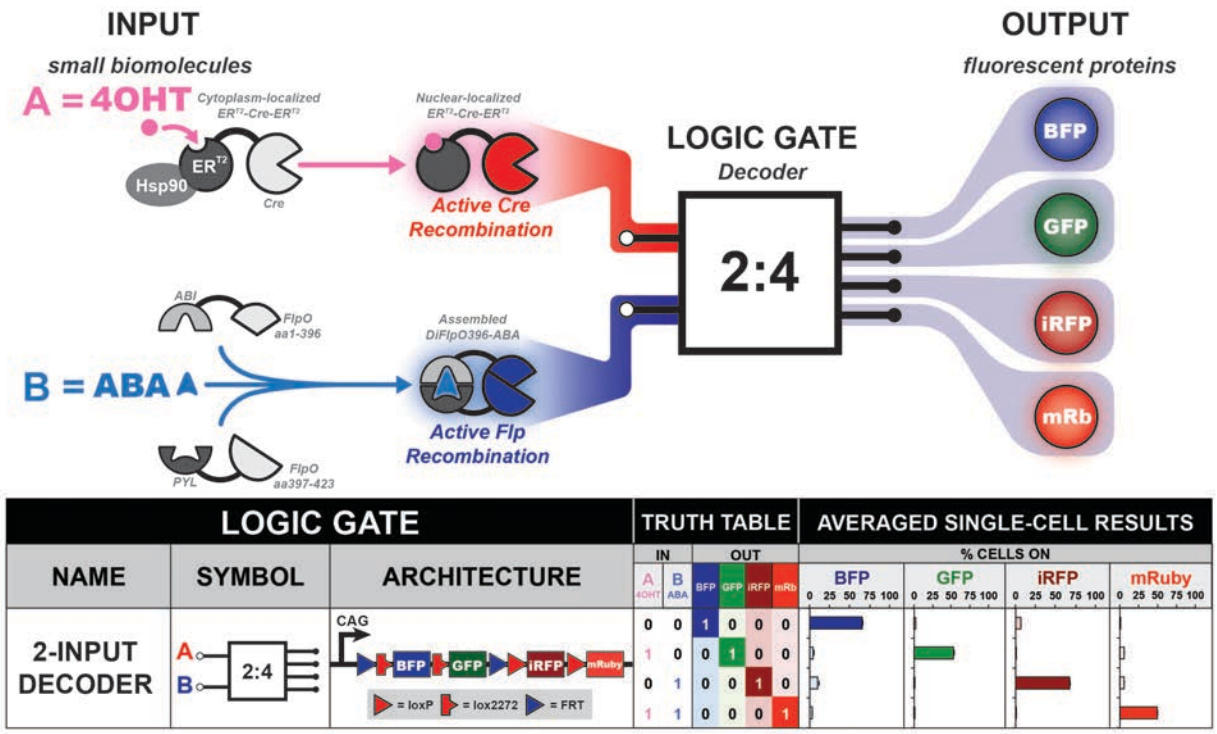

Supplementary Figure 21. Interfacing BLADE with biologically relevant inputs and outputs

Small molecules, 4-hydroxytamoxifen (4OHT) and abscisic acid (ABA), are used to induce Cre and Flp recombination activities, respectively, on a decoder circuit containing four fluorescent protein outputs. Chemical induction of Cre recombination is achieved through 4OHT-mediated translocation of a Cre protein fused to mutated estrogen nuclear receptors (ER^{T2}) from the cytoplasm to the nucleus. Chemical induction of Flp recombination is achieved through a split Flp recombinase construct fused to ABA-binding domains ABI and PYL. Calculated % Cells ON is plotted from n = 3 transfected cell cultures and error bars indicate the standard error of the mean.

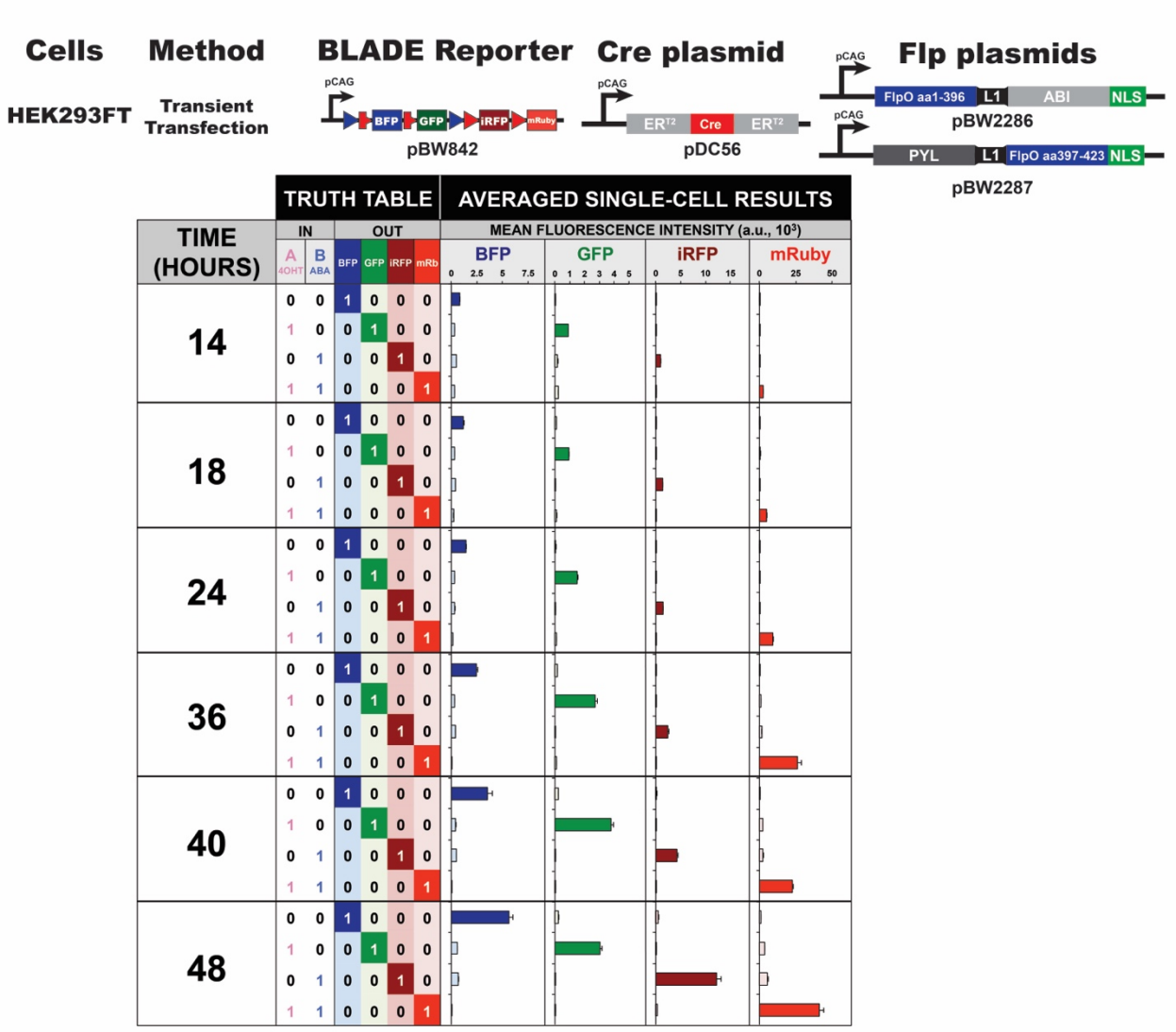

Supplementary Figure 22. Mean fluorescence intensity values for 2-Input 4-hydroxytamoxifen and abscisic acid-inducible decoder in HEK293FT cells over two days represented with histograms

2-Input decoder produces a particular fluorescent protein for each row of the truth table. Error bars indicate standard error of the mean of three transfected cell cultures.

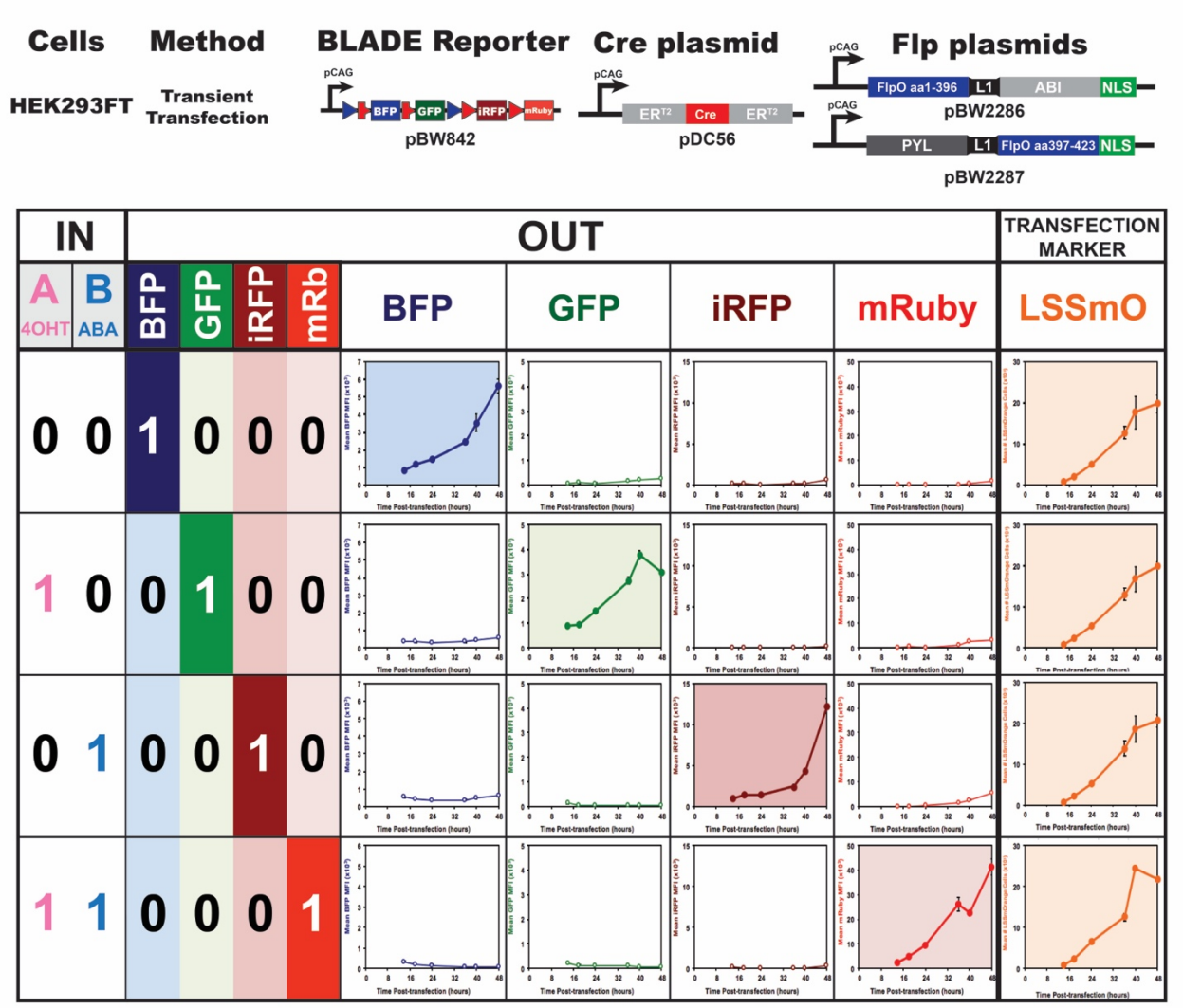

Supplementary Figure 23. Mean fluorescence intensity values for 2-Input 4-hydroxytamoxifen and abscisic acid-inducible decoder in HEK293FT cells over two days represented as a line plot

2-Input decoder produces a particular fluorescent protein for each row of the truth table. Error bars indicate standard error of the mean of three transfected cell cultures.

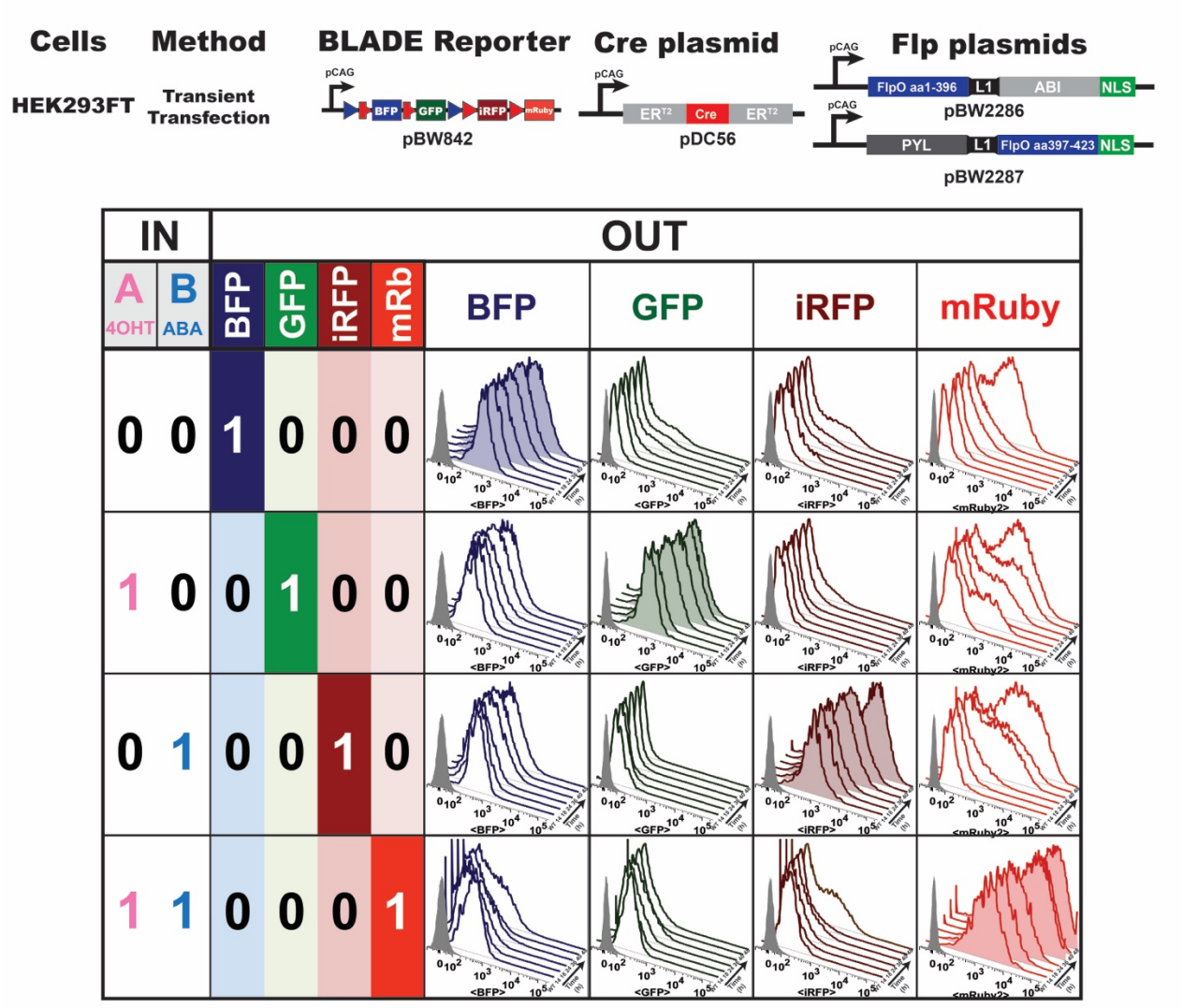

Supplementary Figure 24. Fluorescence histograms for 2-Input 4-hydroxytamoxifen and abscisic acid-inducible decoder in HEK293FT cells over two days

2-Input decoder produces a particular fluorescent protein for each row of the truth table. Grey histograms indicate wildtype HEK293FT, unshaded colored histograms indicate OFF states and shaded colored histograms indicate ON states. Data is shown for one of the transfected cell cultures and for six time points in the z-axis.

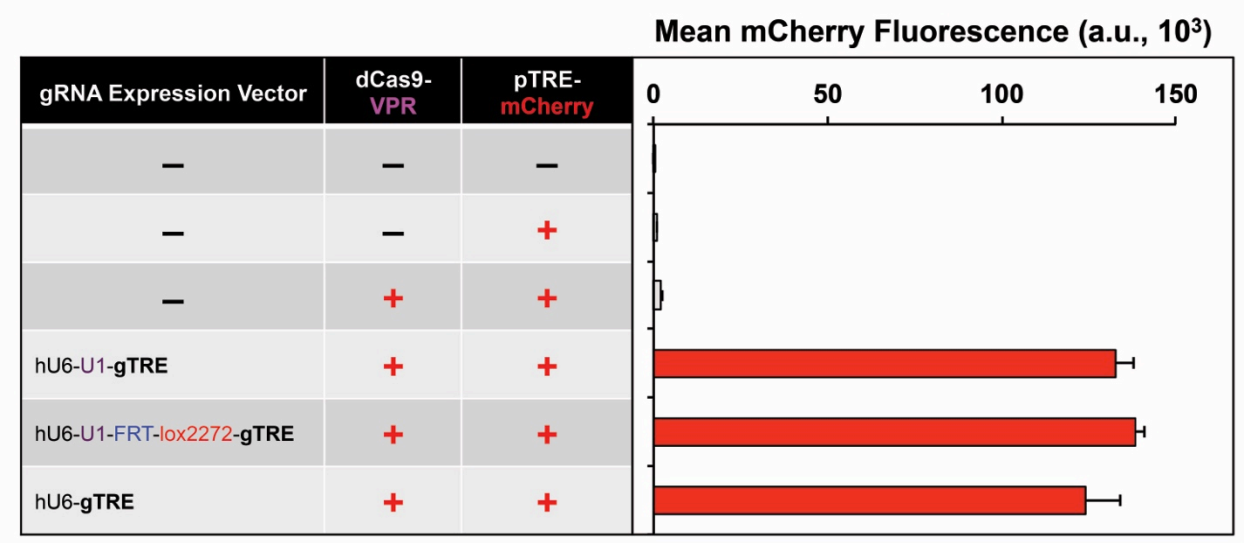

Supplementary Figure 25. 5' recombination site additions do not diminish dCas9-VPR transcription activation

Co-transfection of guide RNA expression plasmids that contain cloning scars (U1 UNS sequence) or FRT and lox2272 sites do not show diminished dCas9-VPR activation of a plasmid containing target sequences upstream a minimal promoter and an mCherry fluorescent protein sequence. Mean fluorescence intensity is from n = 3 transfected cell cultures; a.u. = arbitrary units. Error bars represent standard error of the mean.

a

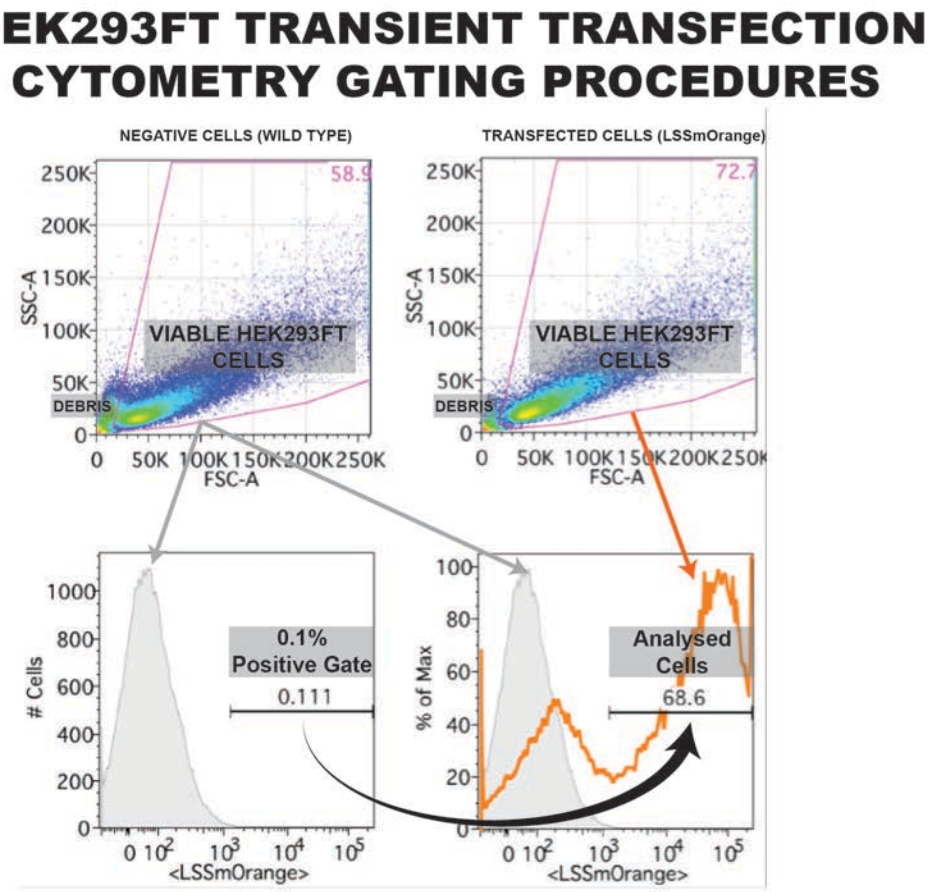

b

COMPENSATION MATRIX

		GFP	mRuby2	BFP	LSSmO	iRFP
		FITC-A	PE-Texas_Red-A	Pacific_Blue-A	LSS_mOrange-A	Alexa_Fluor_700-A
GFP	FITC-A		0	0.8862	5.316	0
mRuby2	PE-Texas_Red-A	0.1436		0.4439	1.063	0.1296
BFP	Pacific_Blue-A	0	0		5.345	0
LSSmO	LSS_mOrange-A	0.1833	0.5717	0.2385		0
iRFP	Alexa_Fluor_700-A	0	0	0	0.1109	

Supplementary Figure 26. Flow cytometric gating procedures for transient transfection of HEK293FT human embryonic kidney cells

(a) Instruments are set initially with an FSC threshold of 500 arbitrary units which filters out a small part of the debris population. All cells are then gated for viable HEK293FT cells as depicted in the pink gates above. Next, a transfection positive gate is made by gating for the top 0.1% transfection marker-expressing (LSS-mOrange or BFP) wild type HEK293FT cells. This gate is then applied to transfected cells and all analyses are done from cells within this gate. (b) An example of a compensation matrix generated through

FlowJo’s auto-compensation tool using single positive fluorescent cells and universal negative wild type cells.

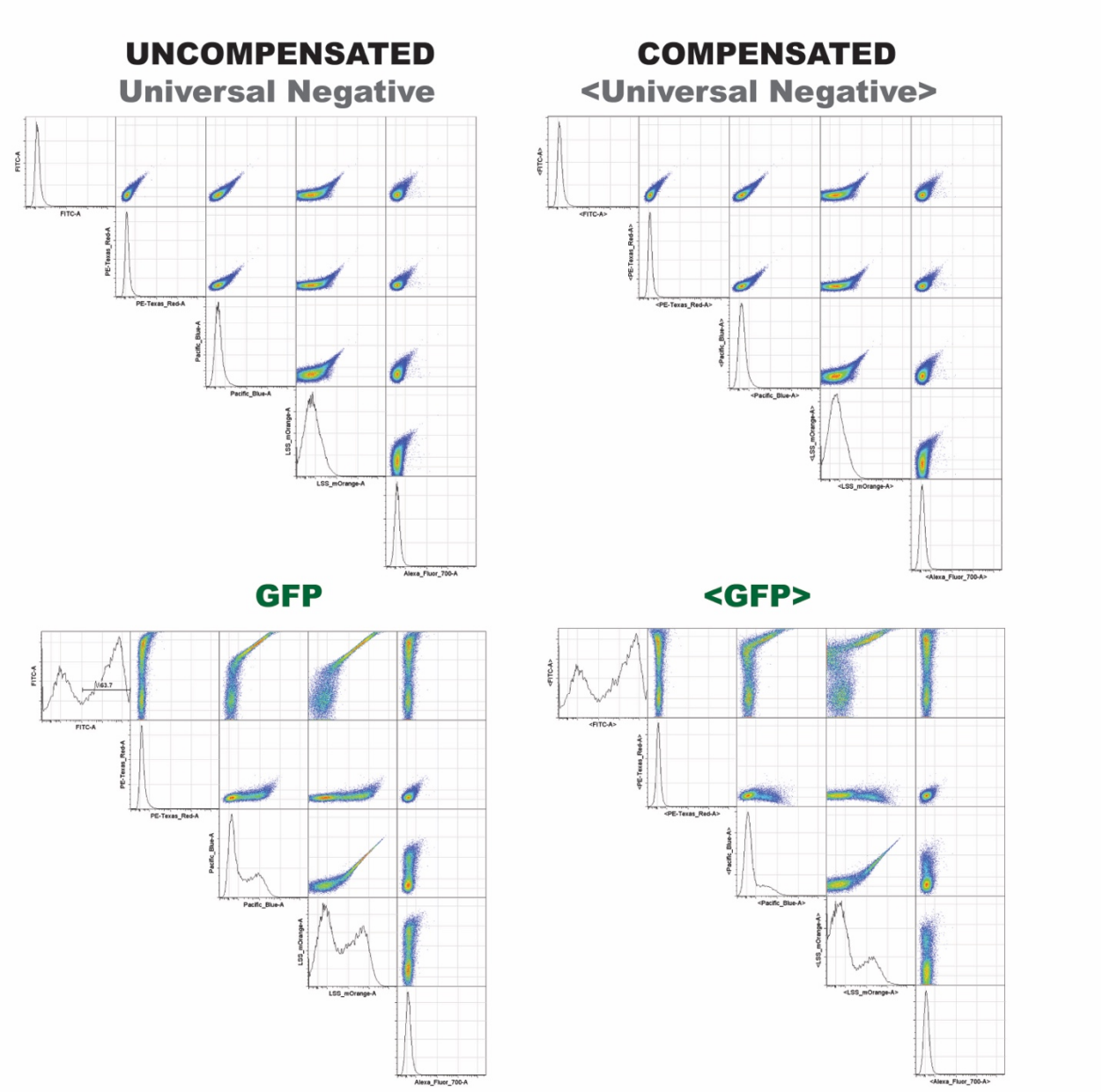

Supplementary Figure 27. Comparison of uncompensated and compensated universal negative and GFP+ HEK293FT cells

Wild type HEK293FT cells are used as a universal negative and cells transfected with pCAG-EGFP are used for GFP+ control.

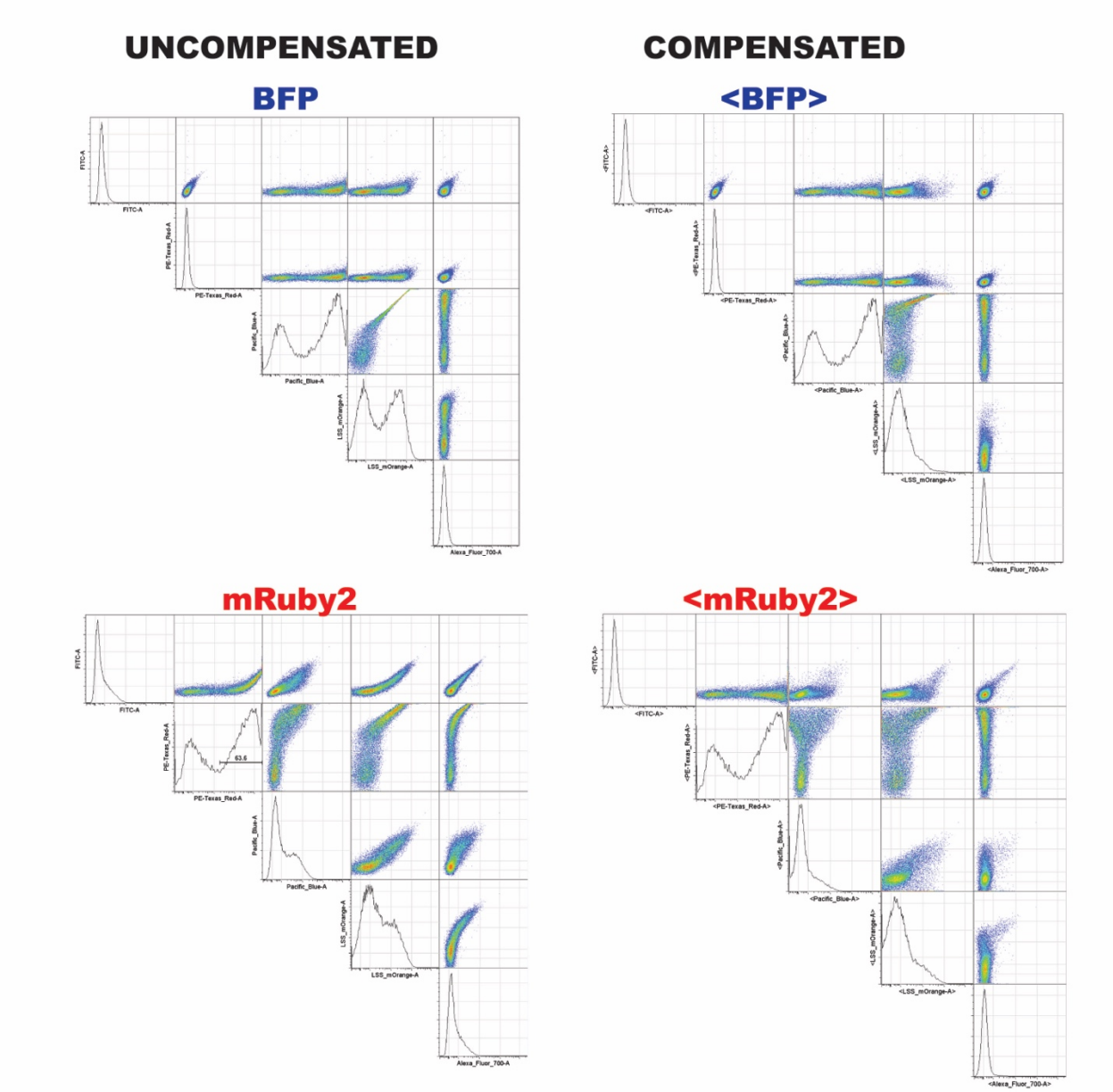

Supplementary Figure 28. Comparison of uncompensated and compensated BFP+ and mRuby2+ HEK293FT cells

Cells transfected with pCAG-tagBFP are used for BFP+ control and cells transfected with pCAG-mRuby2 are used for mRuby2+ control.

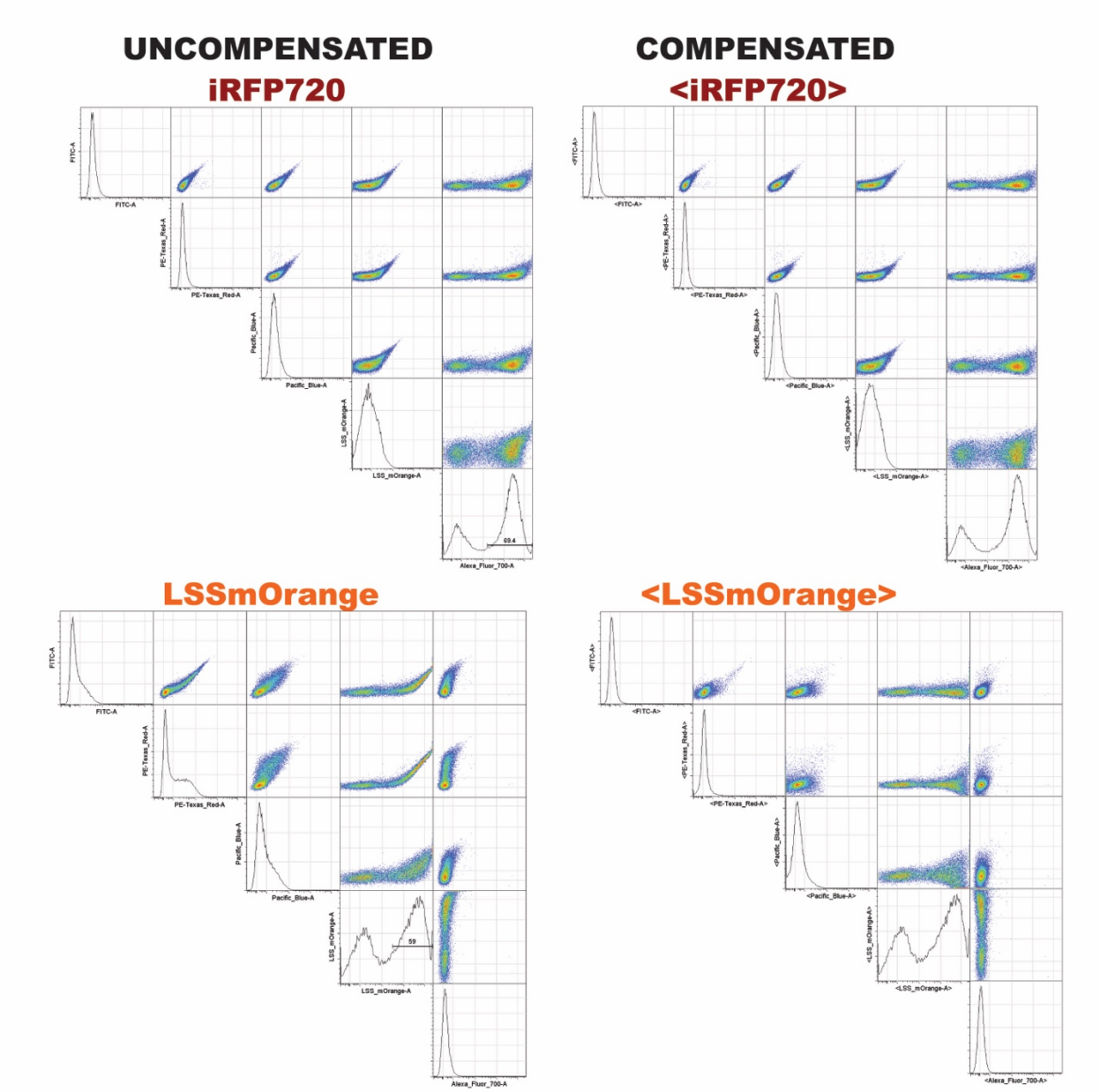

Supplementary Figure 29. Comparison of uncompensated and compensated iRFP+ and LSSmOrange+ HEK293FT cells

Cells transfected with pCAG-iRFP720 are used for iRFP+ control and cells transfected with pCAG-LSSmOrange are used for LSSmOrange+ control.

SUPPLEMENTARY TABLES:

Supplementary Table 1: Setup of buffer gates and recombinase expression plasmids for recombinase cross-reactivity table as detailed in **Figure 1b**, in addition to co-transfection with 62.5ng pCAG-tagBFP (pBW462) and 62.5ng pCAG-FALSE (pBW363).

		loxP	FRT	rox	SloxM1	VloxP	vox	B3RT	KDRT	B2RT	RSRT	φC31 attB/P	bxb1 attB/P	None
	Plasmid ID	pBW338	pBW339	pBW364	pBW271	pBW273	pBW275	pBW276	pBW750	pBW278	pBW279	pBW409	pBW406	pBW363
iCre	pBW390	62.5 ng ea.	62.5 ng ea.	62.5 ng ea.	62.5 ng ea.	62.5 ng ea.	62.5 ng ea.	62.5 ng ea.	62.5 ng ea.	62.5 ng ea.	62.5 ng ea.	62.5 ng ea.	62.5 ng ea.	62.5 ng ea.
FlpO	pBW391	62.5 ng ea.	62.5 ng ea.	62.5 ng ea.	62.5 ng ea.	62.5 ng ea.	62.5 ng ea.	62.5 ng ea.	62.5 ng ea.	62.5 ng ea.	62.5 ng ea.	62.5 ng ea.	62.5 ng ea.	62.5 ng ea.
DreO	pBW431	62.5 ng ea.	62.5 ng ea.	62.5 ng ea.	62.5 ng ea.	62.5 ng ea.	62.5 ng ea.	62.5 ng ea.	62.5 ng ea.	62.5 ng ea.	62.5 ng ea.	62.5 ng ea.	62.5 ng ea.	62.5 ng ea.
SCre	pBW432	62.5 ng ea.	62.5 ng ea.	62.5 ng ea.	62.5 ng ea.	62.5 ng ea.	62.5 ng ea.	62.5 ng ea.	62.5 ng ea.	62.5 ng ea.	62.5 ng ea.	62.5 ng ea.	62.5 ng ea.	62.5 ng ea.
VCre	pBW433	62.5 ng ea.	62.5 ng ea.	62.5 ng ea.	62.5 ng ea.	62.5 ng ea.	62.5 ng ea.	62.5 ng ea.	62.5 ng ea.	62.5 ng ea.	62.5 ng ea.	62.5 ng ea.	62.5 ng ea.	62.5 ng ea.
Vika	pBW434	62.5 ng ea.	62.5 ng ea.	62.5 ng ea.	62.5 ng ea.	62.5 ng ea.	62.5 ng ea.	62.5 ng ea.	62.5 ng ea.	62.5 ng ea.	62.5 ng ea.	62.5 ng ea.	62.5 ng ea.	62.5 ng ea.
B3	pBW435	62.5 ng ea.	62.5 ng ea.	62.5 ng ea.	62.5 ng ea.	62.5 ng ea.	62.5 ng ea.	62.5 ng ea.	62.5 ng ea.	62.5 ng ea.	62.5 ng ea.	62.5 ng ea.	62.5 ng ea.	62.5 ng ea.
KD	pBW436	62.5 ng ea.	62.5 ng ea.	62.5 ng ea.	62.5 ng ea.	62.5 ng ea.	62.5 ng ea.	62.5 ng ea.	62.5 ng ea.	62.5 ng ea.	62.5 ng ea.	62.5 ng ea.	62.5 ng ea.	62.5 ng ea.
B2	pBW437	62.5 ng ea.	62.5 ng ea.	62.5 ng ea.	62.5 ng ea.	62.5 ng ea.	62.5 ng ea.	62.5 ng ea.	62.5 ng ea.	62.5 ng ea.	62.5 ng ea.	62.5 ng ea.	62.5 ng ea.	62.5 ng ea.
R	pBW438	62.5 ng ea.	62.5 ng ea.	62.5 ng ea.	62.5 ng ea.	62.5 ng ea.	62.5 ng ea.	62.5 ng ea.	62.5 ng ea.	62.5 ng ea.	62.5 ng ea.	62.5 ng ea.	62.5 ng ea.	62.5 ng ea.
φC31	pBW440	62.5 ng ea.	62.5 ng ea.	62.5 ng ea.	62.5 ng ea.	62.5 ng ea.	62.5 ng ea.	62.5 ng ea.	62.5 ng ea.	62.5 ng ea.	62.5 ng ea.	62.5 ng ea.	62.5 ng ea.	62.5 ng ea.
bxb1	pBW439	62.5 ng ea.	62.5 ng ea.	62.5 ng ea.	62.5 ng ea.	62.5 ng ea.	62.5 ng ea.	62.5 ng ea.	62.5 ng ea.	62.5 ng ea.	62.5 ng ea.	62.5 ng ea.	62.5 ng ea.	62.5 ng ea.
None	pBW363	62.5 ng ea.	62.5 ng ea.	62.5 ng ea.	62.5 ng ea.	62.5 ng ea.	62.5 ng ea.	62.5 ng ea.	62.5 ng ea.	62.5 ng ea.	62.5 ng ea.	62.5 ng ea.	62.5 ng ea.	62.5 ng ea.

Supplementary Table 2: Transient transfection setup for 2-input, 1-output logic gates detailed in **Supplementary Figure 3**.

Reporter, ng	**Input State A B**	**Enzyme 1, ng** pCAG-iCre (pBW390)	**Enzyme 2, ng** pCAG-FlpO (pBW391)	**Blank, ng** pCAG-FALSE (pBW363)	**Marker, ng** pCAG-tagBFP (pBW462)
Values shown below	**0 0**	0	0	**50**	**25**
	1 0	**25**	0	**25**	**25**
	0 1	0	**25**	**25**	**25**
	1 1	**25**	**25**	0	**25**

Gate	**Plasmid ID**	**ng**
NOR	pBW334	**25**
OR	pBW335	**25**
AND	pBW336	**25**
NAND	pBW337	**25**
A	pBW338	**25**
B	pBW339	**25**
NOTA	pBW340	**25**
NOTB	pBW341	**25**
A IMPLY B	pBW342	**25**
B IMPLY A	pBW343	**25**
A NIMPLY B	pBW344	**25**
B NIMPLY A	pBW345	**25**
XOR	pBW344	**12.5**
	pBW345	**12.5**
XNOR	pBW334	**12.5**
	pBW336	**12.5**
TRUE	pBW361	**25**
FALSE	pBW363	**25**
XOR	pBW448	**25**
XNOR	pBW450	**25**

Supplementary Table 3: Transient transfection setup of six-input AND gate as detailed in **Figure 1c.**

AND GATE, ng pCAG-6AND (pBW479)	**Enzyme 1, ng** pCAG-PhiC31 (pBW440)	**Enzyme 2, ng** pCAG-bxb1 (pBW439)	**Enzyme 3, ng** pCAG-iCre (pBW390)	**Enzyme 4, ng** pCAG-FlpO (pBW391)	**Enzyme 5, ng** pCAG-B3 (pBW435)	**Enzyme 6, ng** pCAG-KD (pBW436)	**Blank, ng** pCAG-FALSE (pBW363)	**Marker, ng** pCAG-tagBFP (pBW462)
150	**0 or 12.5**	**0 or 12.5**	**0 or 12.5**	**0 or 12.5**	**0 or 12.5**	**0 or 12.5**	**Fill to total DNA amount = 250ng**	**25**

Supplementary Table 4: Setup of buffer gates and recombinase expression plasmids for recombinase heterospecificity table as detailed in **Supplementary Figure 4**, in addition to co-transfection with 62.5ng pCAG-tagBFP (pBW462), 62.5ng pCAG-FALSE (pBW363), and 62.5ng corresponding recombinase expression plasmid.

Buffer Gate	pBW	ng
pCAG-**loxP**-STOP-**loxP**-GFP	338	**25**
pCAG-**lox2272**-STOP-**lox2272**-GFP	427	**25**
pCAG-**loxN**-STOP-**loxN**-GFP	428	**25**
pCAG-**loxP**-STOP-**lox2272**-GFP	451	**25**
pCAG-**loxP**-STOP-**loxN**-GFP	452	**25**
pCAG-**lox2272**-STOP-**loxN**-GFP	453	**25**
pCAG-**FRT**-STOP-**FRT**-GFP	339	**25**
pCAG-**F3**-STOP-**F3**-GFP	429	**25**
pCAG-**F14**-STOP-**F14**-GFP	430	**25**
pCAG-**FRT**-STOP-**F3**-GFP	454	**25**
pCAG-**FRT**-STOP-**F14**-GFP	455	**25**
pCAG-**F3**-STOP-**F14**-GFP	456	**25**
pCAG-**VloxP**-STOP-**VloxP**-GFP	273	**25**
pCAG-**Vlox2272**-STOP-**Vlox2272**-GFP	274	**25**
pCAG-**VloxP**-STOP-**Vlox2272**-GFP	331	**25**

Supplementary Table 5: Transient transfection setup for 2-input, 4-output decoder circuit detailed in **Supplementary Figure 12**.

Reporter pEXPRCAG-DECODER (pBW842)	**Input State A B**	**Enzyme 1, ng** pCAG-iCre (pBW390)	**Enzyme 2, ng** pCAG-FlpO (pBW391)	**Blank, ng** pCAG-FALSE (pBW363)	**Marker, ng** pCAG-LSS-mOrange (pBW474)
35.7	**0 0**	0	0	**178.5**	**35.7**
	1 0	**35.7**	0	**142.8**	**35.7**
	0 1	0	**35.7**	**142.8**	**35.7**
	1 1	**35.7**	**35.7**	**107.1**	**35.7**

Supplementary Table 6. Summary of Vector Proximity (VP) angle and global ranks scores for mean fluorescence intensity (MFI) data of the 2-input-2-output logic gate library in **Figure 3** and % Cell ON data in **Supplementary Figure 13** in terms of number of circuits (#) and percentage of circuits (%).

Analysis:	**MFI**		**% CELLS ON**	
VP Global Rank	**#**	**%**	**#**	**%**
0	109	**96.46%**	112	**99.12%**
1	4	3.54%	1	0.88%
>1	0	0.00%	0	0.00%
VP Angle	**#**	**%**	**#**	**%**
<15°	106	**93.81%**	107	**94.69%**

Supplementary Table 7: Transient transfection setup for six-input Boolean Logic Look-up Table genetic device in **Figure 4**.

BOOLEAN LOGIC LUT, ng pEXPRCAG-LUT (pBW829)	**Input State A B**	**Enzyme 1, ng** pCAG-iCre (pBW390)	**Enzyme 2, ng** pCAG-FlpO (pBW391)	**Enzyme 3, ng** pCAG-PhiC31 (pBW440)	**Enzyme 4, ng** pCAG-Vika (pBW434)	**Enzyme 5, ng** pCAG-B3 (pBW435)	**Enzyme 6, ng** pCAG-bxb1 (pBW439)	**Blank, ng** pCAG-FALSE (pBW363)	**Marker, ng** pCAG-tagBFP (pBW462)
75	**0 0**	0	0	**0 or 25**	**0 or 25**	**0 or 25**	**0 or 25**	**Fill to total DNA amount = 250ng**	**25**
	1 0	**25**	0						
	0 1	0	**25**						
	1 1	**25**	**25**						

Supplementary Table 8: Transient transfection setup for 3-input logic gates detailed in **Figure 5b**.

Reporter	**Input State A B C**	**Enzyme 1, ng** pCAG-iCre (pBW390)	**Enzyme 2, ng** pCAG-FlpO (pBW391)	**Enzyme 3, ng** pCAG-VCre (pBW433)	**Blank, ng** pCAG-FALSE (pBW363)	**Marker, ng** pCAG-tagBFP (pBW462)
Values shown below	**0 0 0**	**0**	**0**	**0**	**0**	**62.5**
	1 0 0	**41.7**	**0**	**0**	**83.3**	**62.5**
	0 1 0	**0**	**41.7**	**0**	**83.3**	**62.5**
	0 0 1	**0**	**0**	**41.7**	**83.3**	**62.5**
	1 1 0	**41.7**	**41.7**	**0**	**41.7**	**62.5**
	1 0 1	**41.7**	**0**	**41.7**	**41.7**	**62.5**
	0 1 1	**0**	**41.7**	**41.7**	**41.7**	**62.5**
	1 1 1	**41.7**	**41.7**	**41.7**	**0**	**62.5**

Gate	**Plasmid ID**	**ng**
FULL ADDER	pBW820	**62.5**
FULL SUBTRACTOR	pBW840	**62.5**
HALF ADDER-SUBTRACTOR	pBW841	**62.5**

Supplementary Table 9: Transient transfection setup for inducible fluorescent protein decoder detailed in **Figure 6a**.

Reporter pEXPRCAG-DECODER (pBW842)	**4OHT (1µM)**	**ABA (100µM)**	**Recombinase Constructs**	**Blank, ng** pCAG-FALSE (pBW363)	**Marker, ng** pCAG-LSS-mOrange (pBW474)
35.7	**0**	**0**	**35.7ng** each**:** pDC56 (**pCAG-ERT2-Cre-ERT2**), pBW2286 (**pCAG-Flp1-396-ABI**), pBW2287 (**pCAG-PYL-Flp397-423-ABI**)	**71.4**	**35.7**
	1	**0**			
	0	**1**			
	1	**1**			

Supplementary Table 10: Transient transfection setup for CRISPR decoder detailed in **Figure 6b**.

Reporter pEXPRCAG-CRISPR-DECODER (pBW842)	**4OHT (1µM)**	**ABA (100µM)**	**Recombinase Constructs**	**CMV-dCas9-VPR (Addgene: 63798)**	**Blank, ng** pCAG-FALSE (pBW363)	**Marker, ng** pCAG-GFP (pBW361)
35.7	**0**	**0**	**35.7ng** each**:** pDC16 (**pSFFV-ERT2-Cre-ERT2**), pBW2286 (**pCAG-Flp1-396-ABI**), pBW2287 (**pCAG-PYL-Flp397-423-ABI**)	**35.7**	**35.7**	**35.7**
	1	**0**				
	0	**1**				
	1	**1**				

Supplementary Table 11: Guide RNA target sequences and quantitative real-time PCR primers. Human guide RNAs and qPCR primers were adapted from [2].

NAME:	SEQUENCE (5' to 3'):
gTRE	ATCGTTCTCTATCACTGATA
gNGN2	GGCGGTGGCGGGGGAGGAGG
gMIAT	GCGCCCATGAAATTTTAATG
gACTC1	TGGCGCCCTGCCCTCTGCTG
gTTN	CCTTGGTGAAGTCTCCTTTG
β-actin Forward	CATGTACGTTGCTATCCAGGC
β-actin Reverse	CTCCTTAATGTCACGCACGAT
NGN2 Forward	TGGGTCTGGTACACGATTGC
NGN2 Reverse	GGGTCTCGATCTTGGTGAGC
MIAT Forward	TGGCTGGGGTTTGAACCTTT
MIAT Reverse	AGGAAGCTGTTCCAGACTGC
ACTC1 Forward	ATGTGTGACGACGAGGAGAC
ACTC1 Reverse	CACGATGGACGGGAAGAC
TTN Forward	TGTTGCCACTGGTGCTAAAG
TTN Reverse	ACAGCAGTCTTCTCCGCTTC

Supplementary Table 12: Comparison between BLADE and recent recombinase-based circuit designs or the large-scale circuit design platform Cello.

Key Attributes	BLADE	Siuti et al.[3]	Bonnet et al.[4]	Roquet et al.[5]	Hsiao et al.[6]	Nielsen et al.[7]
Host Organism	*H. sapiens*	*E. coli*	*E. coli*	*E. coli*	*E. coli*	*E. coli*
Operation	Segment Excision	Part Inversion	Terminator Inversion	Segment Excision/Inversion	Part Excision/Inversion	Promoter Repression
Computing Resource	Recombinase					Transcription Factor
Fundamental Building Block	Line decoder circuit	N/A				NOR/NOT gates
Device Design Algorithm	Recursive algorithm based on # of inputs[a]	Ad hoc for each circuit[b]	Ad hoc for each circuit	Exhaustive search[c]	Ad hoc for each circuit	Heuristic search[d]
Number of functional and distinct circuits shown	>110	~20	~10	~5	1	~60
Metric (% success)	Yes (>93%)[e]	No				Yes (75%)
Maximum # of inputs shown	6	2	2	3	2	3
Maximum # of transcriptional outputs from one circuit shown	4	1	1	3-5[f]	2	1
Types of outputs	ORF, gRNA	ORF	ORF	ORF	ORF	ORF

a. Circuits with more inputs can be designed systematically with a recursive strategy that insert the BLADE circuit into another 1-input recombinase circuit (**Supplementary Figure 20**).
b. Each circuit has a unique design approach.
c. All possible circuit permutations are based on available recombination sites are computationally evaluated.
d. Circuit design is based on characterized parts and prior experimental results.
e. 93.81% of circuits have a VP angle of ≤ 15°. 96.46% of circuits have a VP global rank equal to 0.
f. Some of the circuits can display up to 16 states, but only a subset of them can produce transcription outputs.

SUPPLEMENTARY REFERENCES

1 Torella, J. P. *et al.* Unique nucleotide sequence-guided assembly of repetitive DNA parts for synthetic biology applications. *Nature protocols* **9**, 2075-2089, doi:10.1038/nprot.2014.145 (2014).

2 Chavez, A. *et al.* Highly efficient Cas9-mediated transcriptional programming. *Nature methods* **12**, 326-328, doi:10.1038/nmeth.3312 (2015).

3 Siuti, P., Yazbek, J. & Lu, T. K. Synthetic circuits integrating logic and memory in living cells. *Nature biotechnology* **31**, 448-452, doi:10.1038/nbt.2510 (2013).

4 Bonnet, J., Yin, P., Ortiz, M. E., Subsoontorn, P. & Endy, D. Amplifying genetic logic gates. *Science* **340**, 599-603, doi:10.1126/science.1232758 (2013).

5 Roquet, N., Soleimany, A. P., Ferris, A. C., Aaronson, S. & Lu, T. K. Synthetic recombinase-based state machines in living cells. *Science* **353**, aad8559, doi:10.1126/science.aad8559 (2016).

6 Hsiao, V., Hori, Y., Rothemund, P. W. & Murray, R. M. A population-based temporal logic gate for timing and recording chemical events. *Molecular systems biology* **12**, 869, doi:10.15252/msb.20156663 (2016).

7 Nielsen, A. A. *et al.* Genetic circuit design automation. *Science* **352**, aac7341, doi:10.1126/science.aac7341 (2016).